PENETRATION OF PROTONS, ALPHA PARTICLES, AND MESONS[1,2]

By U. Fano

National Bureau of Standards, Washington, D. C.

[1] The survey of literature pertaining to this review was concluded in March 1963.

[2] This article is related to a "state of the art" survey being conducted by the National Research Council Committee on Nuclear Science, Subcommittee on Penetration of Charged Particles. The forthcoming final report of this survey (87) will contain considerably more detailed information than this article. Members of the Subcommittee are: S. K. Allison, Walter Barkas, Martin J. Berger, Hans Bethe, Hans Bichsel, U. Fano, R. L. Gluckstern, William P. Jesse, Jens Lindhard, L. C. Northcliffe, Robert L. Platzman, R. H. Ritchie, R. M. Sternheimer, J. E. Turner.

Dr. James E. Turner of the Health Physics Division, Oak Ridge National Laboratory, has been collaborating with the author in relevant research work and has helped him materially with the preparation of the article itself. His contribution and that of the Subcommittee members, particularly Dr. R. L. Platzman and Dr. H. Bichsel, are gratefully acknowledged.

1. INTRODUCTION

Since the early work of Rutherford and Bragg, the study of penetration of high energy radiation through matter has been important for nuclear physics, in connection with the analysis of experiments. The penetration also provides information on the properties of the materials traversed, but this important aspect of the phemomenon will be treated as secondary in the present article.

Protons, α particles, and mesons with energies up to the order of 1 GeV traverse matter, in great majority, on an approximately straight path, dissipating their energy gradually through a multitude of inelastic collision processes with atomic electrons. Therefore the penetration depends chiefly on the average energy loss resulting from these collisions (the "stopping power" of the material). Combination of experimental and theoretical results provides values of the stopping power with an accuracy which is currently approaching 1 percent for particle energies above 1 MeV. The total distance traveled by a particle in the course of its penetration ("range" of a particle) is obtained by integrating the reciprocal stopping power over the energy from its initial value down to rest.

At lower particle energies, i.e., at particle velocities comparable to those of outer atomic electrons, capture and loss of electrons by the penetrating particle complicate its energy loss process. Much experimental information on this energy range, within which the stopping power reaches its maximum value, has been developed and reviewed recently [Whaling (137), Allison & Garcia Munoz (87, 88)]. However, systematic analysis and comparison with theory have thus far been scarce in this range [see, e.g., Lindhard & Scharff (85), Lindhard (87)]. Accordingly, this part of our subject will not be treated in the present article. Notice that the stopping power below 1 MeV has little influence on the range of higher energy particles.

Above 1 GeV, the penetration of protons and other heavy particles (except μ mesons) is limited primarily by nuclear collisions. However, the stopping power along the tracks between these collisions remains important and is as well known as at lower energies, except for the disturbing influence of energy straggling.

Large-angle Rutherford scattering in the course of penetration is a rare event, not to be discussed here. Multiple small-angle Rutherford scattering introduces a gradual divergence in an initially parallel beam of heavy charged particles. This phenomenon is now well understood theoretically (11, 83, 112), and has been reviewed comprehensively by Scott (107). It will be considered here only insofar as it reduces the net penetration of the particles, by causing their tracks to depart from straight lines.

The penetration of electrons and positrons is closely related to that of protons with regard to the interaction with atomic electrons, but it is influenced to a much greater extent by Rutherford scattering and X-ray emission, with which we are not concerned. The penetration of ions heavier than the α particle involves electron capture and loss even far above 1 MeV, and is treated separately in an accompanying article (91). The stopping power of α particles (above several MeV), deuterons, and mesons is closely related to that of protons, as stated in Section 2.9.

Accordingly, the present article is concerned primarily with the stopping power for protons and secondarily with the minor effects of straggling and multiple scattering. The subject thus delimited has been covered in a previous article of this series (130), thus emphasis will be placed on developments after 1954. Among these, the principal ones are:†

(*a*) Additional measurements, particularly on proton beams up to 700 MeV and on high energy particle tracks in emulsions, have shown conclusively that the mean excitation energy I (the key parameter of stopping power theory) is close to 10 Z for medium and heavy elements, though larger for lighter elements. This result is explained approximately by theory.

(*b*) An apparent discrepancy between the interpretations of stopping powers at 10–20 MeV and above 200 MeV has been removed by the realization that shell corrections are more important than they were thought to be. This effect has also been accounted for theoretically.

(*c*) Understanding of the theory of stopping power in solids, particularly with regard to polarization effects, has improved appreciably.

(*d*) Analysis of multiple scattering effects has accounted for most, though not all, of the fluctuations in penetration of high energy protons.

Even though the basis of stopping power theory has remained unchanged

† *Note added in proof:* New results and points of view have been emerging rapidly since this article was planned. Some of them are not yet fully assimilated; others are still under development. Notice particularly the contributions by Barkas and Tsytovich outlined in Sec. 2.13 and by Lindhard on shell corrections (p. 35) and on the penetration of slower particles (87).

for a great many years, it appeared desirable to review it in some detail in the present article, in order to place in the proper context the recent progress and the questions that remain unexplored. A brief discussion of phenomena that occur along particle tracks and are incidental to penetration is given in Section 7.

2. The Theory of Energy Loss

The theory of the energy loss of fast charged particles caused by their inelastic collisions with atoms was established by Bohr (25) through a semiclassical procedure. In this procedure collisions are classified according to their impact parameter b, which is, roughly, the distance of closest approach of the incident particle to the center of an atom. The later quantum-mechanical formulation by Bethe (10) classified, instead, the collisions according to their momentum transfer q, which is *observable* in contrast to b. The vector q is a function of the energy transfer E_n and of the deflection θ experienced by the incident particle. (The uncertainty principle introduces a loose inverse correspondence between b and q, namely, $b \sim \hbar/q$.) The Bohr and Bethe theories apply to separate atoms, i.e., to gases. The influence of many atoms interacting simultaneously with an incident particle and with one another ("density effect") was first taken into account by Fermi (45), again through a semiclassical macroscopic procedure. The connection between the Bethe and Fermi theories was worked out more recently [Fano (43)].

The theory attained from the start an accuracy of the order of 10 percent through recognition of the dominant influence of certain simple circumstances. Further improvements depend, however, on numerous detailed factors.

2.1 *Initial formulas.*—The average energy loss per unit pathlength, $-dE/ds$, experienced by a particle traversing a material which consists of separate atoms (or molecules) is related to the cross section for all possible individual collisions by

$$-\frac{dE}{ds} = \Sigma_i N_i \Sigma_n E_{ni}\sigma_{ni} \qquad 1.$$

where σ_{ni} is the cross section for the inelastic collision which raises an atom of type i to an energy level E_{ni} above its ground state,[3] and where N_i is the density of atoms (or molecules) i. If N_i is expressed in atoms per unit volume, $-dE/ds$ is the energy loss per unit distance traveled; if N_i is in atoms per gram, dE/ds is the loss per g/cm^2 of material traversed. The treatment of a solid or liquid material as an aggregate of separate atoms embodies the approximate "additivity rule" of Bragg. Departures from this rule will be discussed in Sections 2.10, 2.11, and 3.1. In the following we shall normally refer to a single kind of atom and omit the index i and the summation over it for simplicity, but such a summation is implied wherever it is relevant. The Σ_n

[3] In plasmas or other systems, where many atoms are not in their electronic ground state, a collision may bring these atoms to a lower energy level, with negative E_{ni}.

includes both the discrete and the continuous spectrum of energy levels. The fluctuations of energy loss ("straggling"), i.e., the departures from the average $-dE/ds$, will be discussed in Section 5.

The cross section σ_n is taken initially, according to Bethe (10), in a form differential with respect to the final momentum $\mathbf{p}'$ of the incident particle (Fig. 1) and in lowest-order ("Born") approximation[4] in the electromagnetic interaction V between the incident particle and the atomic electrons

$$d\sigma_n = \frac{2\pi}{\hbar v} \left| (\mathbf{p}', n \left| V \right| \mathbf{p}, 0) \right|^2 \delta(E' + E_n - E) \frac{d\mathbf{p}'}{h^3} \qquad 2.$$

Here $\mathbf{p}$, E, and v are the initial momentum, kinetic energy, and velocity of the incident particle; $\mathbf{p}'$, E', and v' the corresponding values after the collision; and E_n the energy of the final stationary state of the atom (whose initial energy $E_0 = 0$). The δ function, which imposes energy conservation, yields 1 when integrated over dE'. This differential is contained in $d\mathbf{p}' = p'^2(dp'/dE')dE'd(\cos\theta)d\varphi$, with $dp'/dE' = 1/v'$. Therefore Equation 2 is equivalent to

$$d\sigma_n = \frac{1}{4\pi^2\hbar^4 v v'} \left| (\mathbf{p}', n \left| V \right| \mathbf{p}, 0) \right|^2 p'^2 d(\cos\theta)d\varphi \qquad 3.$$

2.2 *Recoil variables; small recoil approximation.*—The momentum transfer

$$\mathbf{q} = \mathbf{p} - \mathbf{p}' \qquad 4.$$

serves better than $\mathbf{p}'$ itself to classify the collisions because it represents the recoil of an atomic electron in each collision and it relates, at least statistically, to the energy transfer E_n. Even more closely related to E_n is the kinetic energy Q (see Footnote 5) of an unbound electron with momentum $\mathbf{q}$, which is given by

$$Q(1 + Q/2mc^2) = q^2/2m \qquad 5.$$

$$Q \sim q^2/2m \quad \text{(nonrelativistic)} \qquad 5a.$$

In the limit of large q, where the atomic electrons may be regarded as free and initially at rest, Q coincides with E_n.

Because we are dealing with incident particles of mass M much heavier than the electron mass m, we have normally

$$\left(\frac{q}{p}, \frac{p - p'}{p}, \frac{v - v'}{v}\right) \sim \frac{m}{M} \ll 1 \qquad 6.$$

In the following we shall normally disregard the quantities on the left-hand side of this equation. However, Equation 6 holds only under the condition

$$E \ll \frac{M}{m} Mc^2 \qquad 7.$$

[4] This approximation is discussed in Sec. 2.13.

[5] The definition of Q given here coincides with those of Bethe (10) or Uehling (130) only in the limiting cases of high Q and of low Q and low E_n.

which breaks down in the GeV range for muons and at higher energies for other particles.[6] This breakdown will be discussed briefly in Section 2.12.

Under the condition 6, the component of q parallel to p is fixed by the energy conservation (see Eq. 2 and Fig. 1) at

$$q\cdot\hat{p}=\frac{p^2-p'^2}{2p}+\frac{q^2}{2p}\sim p-p'\sim\frac{dp}{dE}E_n=\frac{E_n}{v} \qquad 8.$$

and its perpendicular component may be indicated by $p\theta$, so that

$$q^2=E_n^2/v^2+p^2\theta^2 \qquad 9.$$

The differential on the right-hand side of Equation 3 can now be transformed in part, to yield

$$p'^2d(\cos\theta)=p'^2\theta d\theta=qdq=m(1+Q/mc^2)dQ \qquad 10.$$

and integrated in part ($\int d\varphi=2\pi$) so that Equation 3 becomes

$$d\sigma_n=\frac{m}{2\pi\hbar^4v^2}\left|(p',n\,|\,V\,|\,p,0)\right|^2\left(1+\frac{Q}{mc^2}\right)dQ \qquad 11.$$

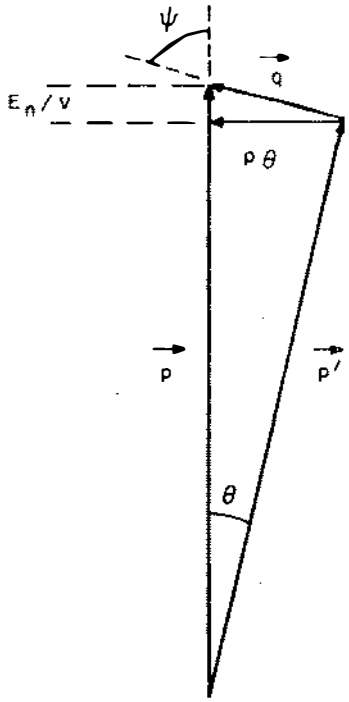

FIG. 1. Momentum transfer diagram in a heavy-particle inelastic collision.

2.3 *Longitudinal and transverse excitations.*—The electromagnetic interaction between the charge and spin, if any, of the incident particle and those of atomic electrons can be subdivided into two terms. One of these consists of the unretarded static Coulomb interaction and the other of the interaction through emission and reabsorption of virtual photons. (This subdivision is called the "Coulomb gauge" representation.) The Coulomb interaction between the incident particle of charge ze at the position $\boldsymbol{r}$ and an atomic electron at $\boldsymbol{r}_j$ can be represented as a Fourier integral $ze^2/|\boldsymbol{r}-\boldsymbol{r}_j|=(ze^2/2\pi^2)\int d\boldsymbol{k}\ k^{-2}\exp[i\boldsymbol{k}\cdot(\boldsymbol{r}_j-\boldsymbol{r})]$. This representation is convenient because, as seen below, each Fourier component with wave vector $\boldsymbol{k}$ serves to transfer the momentum $\hbar\boldsymbol{k}$ from the incident particle to the electron. Alternatively, the same momentum can be transmitted by emission and reabsorption of a photon with momentum $\pm\hbar\boldsymbol{k}$. Emission of a photon of momentum $\hbar\boldsymbol{k}$ by the incident particle is proportional to a matrix element of $zec\boldsymbol{\alpha}\cdot\hat{\mathbf{A}}_s\exp(-i\boldsymbol{k}\cdot\boldsymbol{r})$,

[6] When Eq. 7 breaks down, the energies of an atomic electron and of the incident particle become comparable in their center-of-mass system.

where $zec\boldsymbol{\alpha}$ is the relativistic current operator of the particle and $\hat{\mathbf{A}}_s$ the unit polarization vector of the photon ($s=1$, 2 for two orthogonal directions). The absorption of the same photon by the jth electron is proportional to a matrix element of the corresponding operator $ec\boldsymbol{\alpha}_j \cdot \hat{\mathbf{A}}_s \exp(i\mathbf{k}\cdot\mathbf{r}_j)$. The transmission of the photon with momentum $\pm\hbar\mathbf{k}$ proceeds through an intermediate state whose energy differs from that of the initial and final states by $\hbar ck \pm E_n$. The sum of the contributions of these alternative channels yields the complete interaction matrix element in the form (42)

$$(\ ',n|\ V\ |\ p,0) = \frac{ze^2}{2\pi^2}\int d\mathbf{k}\left\{\frac{(p'|\ e^{-i\mathbf{k}\cdot\mathbf{r}}\ |\ p)(n|\ \Sigma_j e^{i\mathbf{k}\cdot\mathbf{r}_j}\ |0)}{k^2}\right.$$
$$\left. + \Sigma_s \frac{(p'|\ \boldsymbol{\alpha}\cdot\hat{A}_s e^{-i\mathbf{k}\cdot\mathbf{r}}\ |\ p)(n|\ \Sigma_j \boldsymbol{\alpha}_j\cdot\hat{A}_s e^{i\mathbf{k}\cdot\mathbf{r}_j}\ |0)}{k^2-(E_n/\hbar c)^2}\right\} \quad 12.$$

In Equation 12 the matrix elements between momentum eigenstates of the incident particle vanish except when $\mathbf{k}=(\mathbf{p}-\mathbf{p}')/\hbar=\mathbf{q}/\hbar$ (momentum conservation). These matrix elements depend also on spin and other relativistic variables of the particle states, but the square of expression 12 must be summed or averaged over these variables. Under the condition 7 which governs our approximation, this sum or average operation, combined with momentum conservation, is equivalent to setting, in Equation 12,

$$(p'|\ e^{-i\mathbf{k}\cdot\mathbf{r}}\ |\ p) = (2\pi)^3\delta\left(\mathbf{k}+\frac{\mathbf{p}'}{\hbar}-\frac{\mathbf{p}}{\hbar}\right) \quad 13.$$

$$(p'|\ \boldsymbol{\alpha}\cdot\hat{A}_s e^{-i\mathbf{k}\cdot\mathbf{r}}\ |\ p) = \boldsymbol{\beta}\cdot\hat{A}_s(2\pi)^3\delta\left(\mathbf{k}+\frac{\mathbf{p}'}{\hbar}-\frac{\mathbf{p}}{\hbar}\right) \quad 14.$$

where $\boldsymbol{\beta}=\mathbf{v}/c$. We also have

$$\Sigma_s \boldsymbol{\beta}\cdot\hat{A}_s\,\boldsymbol{\alpha}_j\cdot\hat{A}_s = \boldsymbol{\beta}_t\cdot\boldsymbol{\alpha}_j \quad 15.$$

where $\boldsymbol{\beta}_t=\boldsymbol{\beta}-(\boldsymbol{\beta}\cdot\hat{q})\hat{q}$ is the component of $\boldsymbol{\beta}$ perpendicular to $\mathbf{q}$.

As seen in Equation 12, the Coulomb interaction exerts a force parallel to $\mathbf{q}$ and is accordingly called "longitudinal." The interaction through virtual photons is "transverse" because photon fields are perpendicular to $\mathbf{q}$. The Coulomb interaction induces no parity change with respect to reflection on any plane that contains $\mathbf{q}$ because its interaction operator is even under this reflection, whereas the transverse interaction transmits one unit of odd parity with respect to reflection on the plane through $\mathbf{q}$ perpendicular to the $(\mathbf{p}, \mathbf{p}')$ plane. Therefore, any atomic system which is isotropic, i.e., invariant under space rotations and reflections, is excited to states n' and n'' of different parity by the longitudinal and transverse components of the interaction. We deal, then, with separate cross sections $\sigma_{n'}$ and $\sigma_{n''}$ for excitation to different sets of states, even though pairs of levels $E_{n'}$ and $E_{n''}$ often coincide for isolated atoms and molecules [Fano (42)].

In view of these considerations and of expressions 13, 14, 15, and 5, we can now enter Equation 12 into Equation 11 and find

$$d\sigma_n = \frac{2\pi z^2e^4}{mv^2}Z\left\{\frac{|\ F_n(q)\ |^2}{Q^2(1+Q/2mc^2)^2}+\frac{|\ \boldsymbol{\beta}_t\cdot\mathbf{G}_n(q)\ |^2}{[Q(1+Q/2mc^2)-E_n^2/2mc^2]^2}\right\}\left(1+\frac{Q}{mc^2}\right)dQ \quad 16.$$

$$d\sigma_n \sim \frac{2\pi z^2e^4}{mv^2}\frac{dQ}{Q^2}Z|\ F_n(q)\ |^2 \qquad \text{(nonrelativistic)} \quad 16a.$$

where Z is the number of electrons per atom (or molecule),

$$F_n(\boldsymbol{q}) = Z^{-1/2}\Sigma_j(n \mid e^{2\pi i \boldsymbol{q}\cdot\boldsymbol{r}_j/\hbar} \mid 0),$$
$$\boldsymbol{G}_n(\boldsymbol{q}) = Z^{-1/2}\Sigma_j(n \mid \boldsymbol{\alpha}_j e^{2\pi i \boldsymbol{q}\cdot\boldsymbol{r}_j/\hbar} \mid 0) \qquad 17.$$

and where n stands for either n' or n'' with the understanding that either F_n or $\boldsymbol{G}_n$ vanishes for any state of given parity. Notice that the transverse interaction becomes negligible as compared to the electrostatic one in the nonrelativistic limit 16a. The simple structure of Equation 16a is very important. It represents $d\sigma_n$ as the product of $(2\pi z^2e^4/mv^2)dQ/Q^2$, the Rutherford cross section for scattering on a free electron at rest with transfer of the recoil energy $E_n = Q$, of the number Z of atomic electrons, and of a factor (called the "inelastic form factor") which represents the probability of excitation of an atom to the level n if one of its atomic electrons has received a recoil momentum $\boldsymbol{q}$.[7]

For the purpose of applying Equation 16 to the stopping power of isotropic materials, the matrix elements 17 may be regarded as functions only of the magnitude of $\boldsymbol{q}$, i.e. of Q, and of the energy E_n of the final state n, even though they depend formally also on the direction of $\boldsymbol{q}$ and on any orientation characteristics of the states 0 and n. The ground state 0 of an isotropic material has, of course, no orientation characteristics, at least on an average basis. The orientation characteristics of n and of $\boldsymbol{q}$ average out at later stages of the calculation when a summation over the final states n is carried out with a weight function that depends only on E_n, because excited states of an isotropic system with different orientation are degenerate in energy.

[7] The classical derivation of the Rutherford formula for collisions with impact parameter b gives $Q = [(ze^2/b^2)(2b/v)]^2/2m = 2(z^2e^4/mv^2)/b^2$, where ze^2/b^2 is, in essence, the peak force between the charges and $2b/v$ the effective duration of the collision. The Bohr theory (25) was based, in effect, on Eq. 16a even though no method was available in 1913 to calculate $|F_n|^2$. In a sudden collision involving a classical system consisting of many particles, the energy absorbed by the system is the same as though the particles were free. Bohr surmised that this must remain true as a statistical average in a quantum system and, therefore, that the unknown $|F_n|^2$ must be such as to fulfill Equation 27. To calculate completely the nonrelativistic form of 38, Bohr required only the limits to the range of variation of Q. For the upper limit to Q, energy and momentum conservation gave him the correct value (Eq. 20). The lower limit was set by Bohr through the requirement that the collision be sudden, i.e., that its duration $\sim b/v$ remain shorter than the reaction time $\sim\hbar/E_n$ of atomic electrons, since slower ("adiabatic") collisions yield no energy loss. This consideration gives $Q_{\min} \sim z^2e^4/mv^2b_{\max}^2 \sim z^2e^4E_n^2/mv^4\hbar^2 = (ze^2/\hbar v)^2E_n^2/mv^2$, a limit which is less restrictive than the limit (Eq. 18) set by momentum and energy conservation whenever $ze^2/\hbar v < 1$. The limit (Eq. 18) becomes apparent when attention is focused on the momentum transfer rather than on the impact parameter. The stopping power formulas obtained by Bohr and the one obtained later by Bethe (10) are connected by the Bloch formula (18) which reduces to the other two in the limiting cases $ze^2/\hbar v \gg 1$ respectively. The Bohr limit becomes relevant only at low velocities (not considered in this article) at which atomic electrons are normally captured by the incident particle.

2.4 *Mapping on the* (Q, E_n) *plane.*—The inelastic collisions have been classified above in accordance with the energy transfer E_n and recoil parameter Q. The calculation of stopping power involves an integration over these variables. Let us consider the anticipated contribution to the integral from various regions of the (Q, E_n) plane, which are indicated in Figure 2 with logarithmic scales.

Equations 5 and 9 define Q as a monotonic function $Q(E_n, \theta)$. To the limitation $\theta \geq 0$ corresponds

$$Q \geq Q_{\min}(E_n) = Q(E_n, 0) = E_n^2/2mv^2 - \text{relativistic terms} \qquad 18.$$

The full line in Figure 2 represents the function $Q = Q(E_n, 0)$. The integration extends only over points above this line.

The other main relationship between Q and E_n results from the momentum balance in the collision. If an atomic electron were initially free and at rest, a collision with momentum transfer $\boldsymbol{q}$ would send it into the final state with momentum $\boldsymbol{q}$ and energy $E_n = Q$. Therefore, under this idealized, unrealistic circumstance, $F_n(\boldsymbol{q})$ and $\boldsymbol{G}_n(\boldsymbol{q})$ would differ from zero only along the line $Q = E_n$ shown in dashes in Figure 2. In fact, the final state is not uniquely determined by the momentum transfer $\boldsymbol{q}$ from the incident particle to the electron because an atomic electron is subject to forces and thereby exchanges momentum with the rest of the atomic system to which it belongs. Therefore, $F_n(\boldsymbol{q})$ and $\boldsymbol{G}_n(\boldsymbol{q})$ differ significantly from zero throughout a region of the (E_n, Q) plane, on either side of the line $Q = E_n$, which is indicated by the shaded area in Figure 2. The width of this region depends on the magnitude of the likely momentum exchanges between the electron and the rest of its atomic system. As an index of this magnitude we take the mean square momentum of the electron in its initial ground state, since momentum exchanges decrease after the electron moves away from nuclei following the collision. The mean square momentum is $2m\langle K\rangle_0$ in terms of the more familiar mean kinetic energy. It differs, of course, for electrons of different atomic shells, but an average $\langle K\rangle_0$ over all atomic electrons may be considered. More specific information on the statistical correlation between E_n and Q, which results from the values of $F_n(\boldsymbol{q})$ and $\boldsymbol{G}_n(\boldsymbol{q})$, is afforded by inspection of the matrix elements $F_n(\boldsymbol{q})$ calculated for atomic hydrogen (10). From this inspection one obtains a parameter relevant to Figure 2, namely, the variance of the fractional departures of E_n from Q

$$\left\langle \left(\frac{E_n - Q}{E_n + Q} \right)^2 \right\rangle \sim \frac{2\langle K\rangle_0}{E_n + Q} \qquad 19$$

An analogous, more precise, result is given by Equation 69 in Section 5.

Significant values of the cross section $d\sigma_n$ are, therefore, expected to lie within a strip about the line $Q = E_n$ which is very narrow (on the logarithmic scale of Fig. 2) for large E_n and flares out rapidly as E_n decreases to the point of being comparable to $\langle K\rangle_0$.[8] This strip is indicated in Figure 2 by the shaded area.

[8] The flaring out is far more gradual in heavy than in light elements, because of the large spread in the values of $\langle K\rangle_0$ for different shells.

For large values of Q and E_n, the strip lies below the full line in Figure 2, that is, outside the range of integration over Q defined by Equation 18. Therefore, as a result of momentum and energy conservation, no collision occurs with energy loss E_n beyond the intersection of the strip and the full line (except as noted in Sec. 4). The intersection lies at the root of the equation $Q(E_n, 0) = E_n$, namely at $Q = E_n = Q_{max}$, where

$$Q_{max} = 2mv^2/(1 - v^2/c^2) \qquad 20.$$

under the condition 7. The exact value (10) is

$$Q_{max} = 2m(E^2 - M^2c^4)/[(M^2 + m^2)c^2 + 2mE] \qquad 20a.$$

For intermediate values of Q and E_n the strip lies entirely above the line, within the region consistent with Equation 18. Thus the theory need not

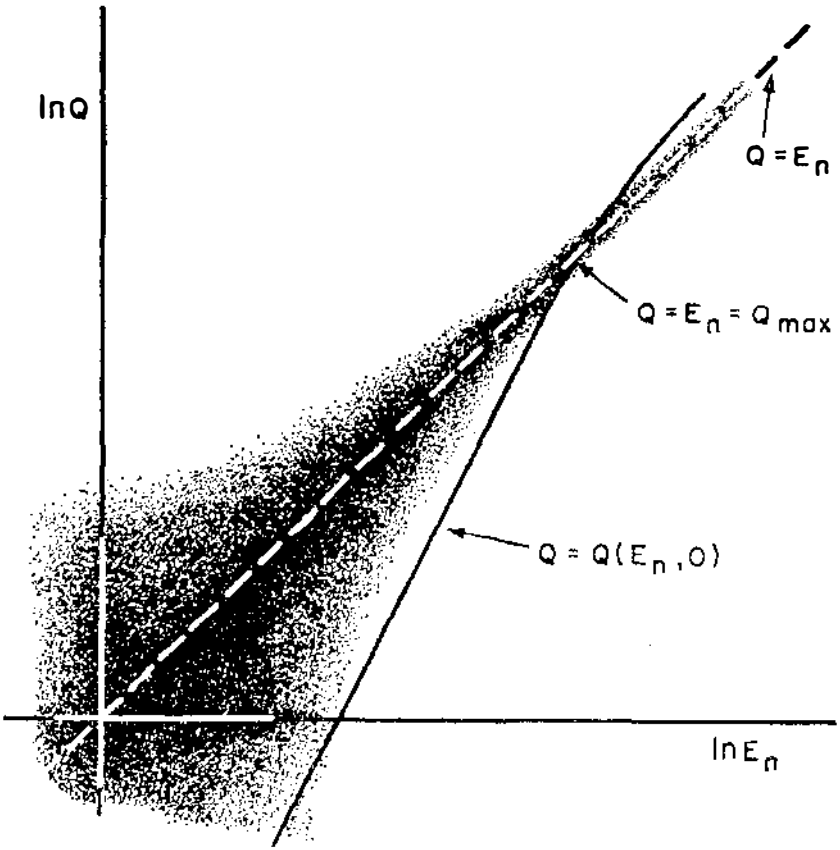

Fig. 2. Diagram of probability distribution of collisions with different values of Q and E_n.

consider the restriction imposed by Equation 18 explicitly in this range, and is thereby greatly simplified. The separation of the strip from the line is characterized graphically by the "empty crescent" between line and strip in Figure 2. The points of the chord of this crescent lie at values of E_n for which

$$\langle K\rangle_0 \ll E_n \ll 2mv^2 \qquad 21.$$

Therefore, the occurrence of the crescent and the simplification resulting from it depend on the condition $\langle K\rangle_0 \ll 2mv^2$, i.e., on the incident particle being much faster than the atomic electrons. Failure of condition 21 leads to a more difficult situation discussed in Section 4.

At low values of E_n the shaded strip reaches down to and below the full line of Figure 2.

Additional remarks can be made about the contribution of transverse excitations to Equation 16. In the first place, β_t and consequently the whole contribution vanish at the limit $\theta=0$, $Q=Q_{\min}$ (i.e., on the full line) because $\boldsymbol{q}$ is parallel to $\boldsymbol{\beta}$ at this limit. (A moving charge does not emit or absorb photons in its own direction.) Therefore, the limit $Q=Q_{\min}$ need not appear explicitly in the integrated contribution of transverse excitations to stopping power, as will be verified in Section 2.8. Secondly, the denominator of the second term in Equation 16 increases rapidly as Q increases, without any compensating increase of $\boldsymbol{G}_n(\boldsymbol{q})$ in the numerator. As a result, values of $Q \gg Q_{\min}$ contribute little to transverse excitations. These excitations are thus confined to a narrow strip parallel to the full line in Figure 2 lying a little above it. This strip lies within the shaded strip only at low Q and again at high Q. The lack of points common to the two strips at intermediate Q means that transverse interactions can be disregarded here. This circumstance has facilitated the theory (10).

2.5 *Low-Q approximation.*—In the range of low Q, the matrix elements $F_n(q)$ and $\boldsymbol{G}_n(\boldsymbol{q})$ can be evaluated by expanding the exponential within them into powers of $\boldsymbol{q}$ to the lowest nonvanishing order, namely, q^1 for F_n and q^0 for $\boldsymbol{G}_n$. The expansion assumes that $\hbar/q$ is much larger than the linear dimension of the atomic system under consideration; it does not hold for macroscopic amounts of condensed matter that behave as a single atomic system and are treated separately in Section 2.10 and 2.11.

The matrix elements F_n and $\boldsymbol{G}_n$ reduce, in this approximation, to dipole and velocity matrix elements, respectively. Moreover, the velocity element equals the dipole element times $iE_n/\hbar$. One finds thus

$$|F_n(q)|^2 \sim Z^{-1}q^2 \left|(\Sigma_j x_j)_{n0}\right|^2/\hbar^2 = Qf_n/E_n \qquad 22.$$

$$|\boldsymbol{\beta}_t\cdot\boldsymbol{G}_n(q)|^2 \sim Z^{-1}\beta_t^2 E_n^2 \left|(\Sigma_j y_j)_{n0}\right|^2/\hbar^2c^2 = \beta_t^2 f_n E_n/2mc^2 \qquad 23.$$

where x_j, y_j are electron coordinates in the directions of $\boldsymbol{q}$ and $\boldsymbol{\beta}_t$, respectively, and f_n is the optical dipole oscillator strength for excitation to the level n.[9]

[9] The oscillator strength is defined
leads to 33 instead of $\Sigma_n f_n = Z$.

Substitution of Equations 22 and 23 into the $d\sigma_n$ given by Equation 16 makes this expression easy to sum over n and integrate over Q. In the transverse excitation term, Q can be replaced by

$$\cos^2\psi = \frac{q_{\min}^2}{q^2} = \frac{Q_{\min}(Q_{\min} + 2mc^2)}{Q(Q + 2mc^2)} \qquad 24.$$

where ψ is the angle between p and q. This yields

$$E_n d\sigma_n \sim \frac{2\pi z^2 e^4}{mv^2} Z f_n \left\{ \frac{dQ}{Q} + \beta^4 \frac{\sin^2\psi}{(1-\beta^2\cos^2\psi)^2} d(\cos^2\psi) \right\} \qquad 25.$$

2.6 *Intermediate-Q range.*—This is the range in which the shaded area in Figure 2 is detached from the line $Q = Q_{\min}$ and in which the contribution of transverse excitations is assumed to be negligible. Detachment from the limit of integration over Q—which depends on E_n—enables one to calculate contributions to stopping power by carrying out the sum over the levels n for each value of Q. Dropping the transverse term in Equation 16 as well as relativistic corrections of order Q/mc^2, we obtain from Equation 16

$$\Sigma_n E_n d\sigma_n = \frac{2\pi z^2 e^4}{mv^2} Z \frac{dQ}{Q^2} \Sigma_n E_n \left| F_n(q) \right|^2 \qquad 26.$$

There is no need here to evaluate $\left| F_n(q) \right|^2$ itself, since a sum rule given by Bethe (10) (a generalization of $\Sigma_n f_n = 1$) yields

$$\Sigma_n E_n \left| F_n(q) \right|^2 = Q \qquad 27.$$

With reference to the interpretation of $\left| F_n \right|^2$ at the end of Section 2.3, the important result 27 means that, when atomic electrons receive a momentum q, they absorb on the average the same amount of energy Q as though they had been free and at rest, regardless of atomic binding and of the spectrum of energy levels E_n.[7]

Relativistic corrections Q/mc^2 have been dropped in the expectation that the high-Q approximation holds whenever $Q/mc^2 \ll 1$ fails. It has also been implied in Equation 27 that Q (or q) is sufficiently low to insure that relativistic values of E_n do not contribute appreciably to the sum. Indeed, Equation 27 rests on the assumed use of nonrelativistic wave functions in the matrix elements F_n. These assumptions break down, in fact, for the excitation of K-shell electrons in heavy elements, and are not very accurate for L electrons in heavy atoms or for the K electrons of medium-heavy elements. The errors incurred by the stopping power theory on account of this inaccuracy do not appear to have been studied extensively, but Perlman (94) found the stopping power of the mercury K electrons for incident 1-MeV electrons to be twice as large as predicted by a nonrelativistic calculation.[10] Even though Equation 26 introduces such a substantial error in the contri-

[10] According to Perlman, the ejection of K electrons by electron collisions shows relativistic effects of 10–20 percent even for incident energies ~50 keV and binding energies ~8 keV. Analysis of this calculation might be an initial step to a serious study of the upper limit of the intermediate-Q approximation.

bution of individual electrons to the stopping power, the total error may not exceed the order of 1 percent because the innermost shells contain only a small fraction of the electrons of heavy elements.

2.7 *High-Q approximation.*—When $Q \gg \langle K \rangle_0$, the mean kinetic energy that represents the effect of atomic binding in Equation 19, E_n cannot depart much from Q. One disregards, then, this departure, and the binding responsible for it, and evaluates the matrix elements $F_n(q)$ and $\boldsymbol{G}_n(q)$ (Eq. 17) as though the initial and final electron states were free-particle momentum eigenstates, with momenta $\boldsymbol{p}_0 = 0$ and $\boldsymbol{p}_n = \boldsymbol{q}$. This evaluation, carried out with Dirac relativistic wave functions and with appropriate averaging or sum over alternative spin orientations, yields

$$\begin{aligned} |F_n(q)|^2 &\sim \frac{1 + Q/2mc^2}{1 + Q/mc^2}\delta_{nq} \\ |\beta_t \cdot \boldsymbol{G}_n(q)|^2 &\sim \beta_t^2 \frac{Q/2mc^2}{1 + Q/mc^2}\delta_{nq} \end{aligned} \qquad 28.$$

where the Kronecker δ indicates that the matrix elements vanish unless the state n is an eigenstate of momentum $\boldsymbol{q}$. Substitution into Equation 16 gives

$$\Sigma_n E_n d\sigma_n = \frac{2\pi z^2 e^4}{mv^2} Z \left\{ \frac{1}{Q(1 + Q/2mc^2)} + \frac{\beta_t^2}{2mc^2} \right\} dQ \qquad 29.$$

Notice that this expression reduces to the "intermediate-Q" results (Eqs. 26, 27), in the nonrelativistic limit $Q \ll mc^2$. No separate high-Q approximation is, therefore, required for $\beta \ll 1$. On the other hand, the contribution of transverse interaction predominates in the opposite limit $Q \gg mc^2$. Part of the dependence of Equation 29 on Q is included in

$$\beta_t^2 = \beta^2(1 - q_{\min}^2/q^2) = (1 + Q/2mc^2)^{-1} - (1 - \beta^2) \qquad 30.$$

Substitution of Equation 30 into Equation 29 allows one to combine the longitudinal and transverse contributions[11] to yield

$$\Sigma_n E_n d\sigma_n = \frac{2\pi z^2 e^4}{mv^2} Z \left(\frac{1}{Q} - \frac{1 - \beta^2}{2mc^2} \right) dQ \qquad 31.$$

2.8 *The basic stopping power formula.*—The stopping power theory leans heavily on the possibility of piecing together the low-, intermediate- and high-Q approximations. For this purpose we assume that a value Q_1 of Q exists at which the results of both Sections 2.5 and 2.6 are applicable and another value Q_2 exists at which Sections 2.6 and 2.7 hold. Shortcomings of this assumption will be discussed below.

In the low-Q range we integrate Equation 25 from $Q_{\min}$, as given by Equation 18, to Q_1 and over $\cos^2\psi$ from 0 to 1 and find

$$E_n \int_{Q_{\min}}^{Q_1} d\sigma_n = \frac{2\pi z^2 e^4}{mv^2} Z f_n \left\{ \ln \frac{Q_1}{E_n^2/2mv^2} + \ln \frac{1}{1 - \beta^2} - \beta^2 \right\} \qquad 32.$$

[11] Heretofore, calculations have given 31 directly without prior separation of longitudinal and transverse contributions.

The remaining summation over n is trivial for the terms that contain only f_n, owing to the Thomas-Kuhn sum rule

$$\Sigma_n f_n = 1 \tag{33.}$$

The sum over the term with $\ln E_n$ is represented by means of an important atomic parameter, the mean excitation energy I, which is a logarithmic mean over the excitation energies E_n weighted according to the corresponding oscillator strengths f_n and is defined by[12]

$$\ln I = \Sigma_n f_n \ln E_n \tag{34.}$$

Equations 32, 33, and 34 yield, then,

$$\Sigma_n E_n \int_{Q\min}^{Q_1} d\sigma_n = \frac{2\pi z^2 e^4}{mv^2} Z \left\{ \ln \frac{Q_1 2mv^2}{I^2} + \ln \frac{1}{1-\beta^2} - \beta^2 \right\} \tag{35.}$$

In the intermediate range, Equations 26 and 27 lead directly to

$$\int_{Q_1}^{Q_2} \Sigma_n E_n d\sigma_n = \frac{2\pi z^2 e^4}{mv^2} Z \ln \frac{Q_2}{Q_1} \tag{36.}$$

In the high-Q range, Equation 29 is to be integrated from Q_2 to the upper limit $Q_{\max}$[13] given by Equation 20. The expression 30 of β_i^2 is to be used and Q_2/mc^2 disregarded, in keeping with the intermediate-Q approximation. This yields

$$\int_{Q_2}^{Q_{\max}} \Sigma_n E_n d\sigma_n = \frac{2\pi z^2 e^4}{mv^2} Z \left\{ \ln \frac{2mv^2}{Q_2} + \ln \frac{1}{1-\beta^2} - \beta^2 \right\} \tag{37.}$$

where the last two terms in the braces arise from the transverse excitations[14] and are identical to the corresponding contribution to Equation 35.

The sum of Equations 35, 36, and 37, multiplied by N in accordance with Equation 1, gives the complete stopping power to within corrective factors indicated by C/Z and δ and discussed below. We write

$$\begin{aligned} -\frac{dE}{ds} &= N\Sigma_n E_n \int_{Q_{\min}}^{Q_{\max}} d\sigma_n \\ &= \frac{2\pi z^2 e^4}{mv^2} NZ \left\{ \ln \frac{(2mv^2)^2}{I^2} + 2 \ln \frac{1}{1-\beta^2} - 2\beta^2 - 2\frac{C}{Z} - \delta \right\} \\ &= \frac{4\pi z^2 e^4}{mv^2} NZ \left\{ \ln \frac{2mv^2}{I} + \ln \frac{1}{1-\beta^2} - \beta^2 - \frac{C}{Z} - \tfrac{1}{2}\delta \right\} \end{aligned} \tag{38.}$$

[12] The energy I is often treated in the literature as an adjustable parameter of stopping power theory, which may depend on the velocity of the incident particle. Here, as in (10) and (130), it is treated as a property of each material defined by Eq. 34, regardless of the kind and speed of the incident particle, even though its numerical value may not be well known and is in practice commonly obtained by fitting the theory to experimental results.

[13] The integration would extend to $Q = \infty$ in principle, but the approximation introduced in Sec. 2.7 requires the introduction of a cutoff at $Q_{\max}$.

[14] Integration of Eq. 31 instead of Eq. 29 leads to a form of Eq. 37 with the first two terms in the braces combined to yield $\ln (Q_{\max}/Q_2)$.

and note that

$$4\pi z^2 e^4 NZ/mv^2 = 0.307\beta^{-2} z^2 Z/A \text{ MeV/g cm}^{-2} \quad 38a.$$

where A is the chemical atomic weight.

Notice that Q_1 and Q_2, introduced to delimit the three approximation ranges, cancel out in the sum.

The stopping power formula 38 is the product of two factors. The first, in front of the braces, is a monotonically decreasing function of the incident particle's velocity. The second, in the braces, is a slowly (logarithmic) monotonically increasing function of the particle's energy. The second factor's influence predominates only at very low energies, below 1 MeV, where the logarithmic rise is comparatively fast, and at extremely high energies, where the first factor approaches its limiting value ($v^2 \sim c^2$). The stopping power increase at high energies stems from the transverse interaction and is called the "relativistic rise." This rise diverges logarithmically in the high energy limit, but the diverging term requires some modification and some reinterpretation, to be discussed in Sections 2.11 and 2.12. In the intermediate energy range, from less than 1 MeV to more than 1 GeV for protons, the first factor's influence predominates and causes the stopping power to decrease with increasing energy of the incident particle.

The principal nontrivial factor in the theoretical evaluation of the stopping power for each material thus becomes the determination of the average excitation energy I. This problem will be treated in Section 3. The remaining problems concern inaccuracies of the approximations utilized in the derivation of Equation 38. Of course, even sizable errors incurred at specific points of the calculation may have only a minor influence on the integral 38.

The chief inaccuracy lies often at the junction of the low-Q and intermediate-Q approximations. The existence of a Q_1, at which both approximations hold, depends on the validity of the low-Q formulas 22 and 23 all along the line $Q = Q_{\min}$, defined by expression 18, until it emerges from the strip defined by Equation 19. The low-Q formulas hold for $Q \ll \langle K \rangle_0$ and $Q \ll E_n$, conditions which are fulfilled by the relevant values of Q and E_n provided Equation 21 is satisfied, that is, provided the incident particle is much faster than the atomic electrons. This condition is actually satisfied for high energies of incidence and for the majority of atomic electrons, but it fails increasingly for inner electrons and at lower energies of incidence. The modifications required by this failure, called "inner shell corrections," are represented by C/Z in Equation 38 and are treated in Section 4.

Inaccuracies arising from inadequate overlapping of the intermediate and high-Q approximations at $Q = Q_2$ have not been studied, as noted in Section 2.6. They include the possible effect of transverse excitations in this range and result, like the inaccuracies at $Q = Q_1$, from the high speed of inner shell electrons in heavy atoms.

Other appreciable corrections stem from the "density effect," that is, from modifications to the low-Q formulas 22 and 23 which are required for application to condensed materials (see Sec. 2.10, 2.11). They involve a

more careful definition of the parameter I and the introduction of δ in Equation 38.

2.9 *Range formula.*—The range of a particle of given initial kinetic energy E_0 traversing a given material is variously defined as the mean pathlength covered by it before coming to rest or the mean distance traveled in its initial direction (depth of penetration). These two definitions differ somewhat on account of small deflections of the particle track, to be discussed in Section 6. In this article "range" means the mean pathlength, and the depth of penetration will be called "projected range." Normally it is sufficient to evaluate the mean pathlength in the continuous slowing down approximation (Sec. 5) which yields the result, to be called "c.s.d.a. range" in accordance with (87),

$$R(E_0) = \int_0^{E_0} \frac{dE}{-dE/ds} \qquad 39.$$

Poor knowledge of the stopping power at low energies, $E < 1$ MeV, causes little uncertainty in $R(E_0)$ for $E_0 \gg 1$ MeV, since the interval $E < 1$ MeV corresponds to large values of $-dE/ds$ and thus contributes little to the integral. In practice it is convenient to separate the interval of integration in Equation 39 into a small part, $0 < E < E_1 \sim 1$ MeV, whose contribution is taken from experimental data, and a large one, $E_1 < E < E_0$, which can be obtained from theory.

The stopping power, as given by Equation 38, depends on the particle's kinetic energy only through its velocity. Therefore it is a function of E/M, where M is the particle's mass. The stopping power is also proportional to the squared charge of the particle z^2e^2. These circumstances enable one to obtain the range functions of different particles from one another by a scaling operation, at least within the approximation 38. If we call $S_p(E)$ the stopping power (Eq. 38) of a given material for protons, the stopping power for another heavy particle of charge ze and of mass M, *in units of the proton mass*, is $z^2 S_p(E/M)$ and its range will be

$$R(E_0) = \int_0^{E_0} \frac{dE}{z^2 S_p(E/M)} = \frac{M}{z^2} \int_0^{E_0/M} \frac{d(E/M)}{S_p(E/M)} = \frac{M}{z^2} R_p\left(\frac{E_0}{M}\right) \qquad 40.$$

This scaling operation does not apply to the onset of corrections for electron capture and loss at low particle energies. These corrections depend on the value of $ze^2/\hbar v$, the velocity ratio for a captured electron and the particle, and thus set in at higher velocity for α particles ($z = 2$) than for protons. They can be applied by separating out the integration over the low energy interval as noted above (see also Sec. 8.3).

The current availability of range tables is discussed in Section 8. The c.s.d.a. range considered here coincides with the most probable pathlength only if the pathlength fluctuations, called "straggling," are symmetric about the mean. Departures from symmetry may be appreciable (see Sec. 5), especially when one deals with partial ranges, that is, with the mean path-

length $R(E_0)-R(E_1)$ traversed within a given small energy interval from E_0 to E_1.

2.10 *Low-Q longitudinal excitations in condensed materials.*—The basic low-Q approximation formula 22 for longitudinal excitations involves an expansion of exp $(i\boldsymbol{q}\cdot\boldsymbol{r}/\hbar)$ into powers of $\boldsymbol{q}$. Practical use of this expansion implies that the positions $(\boldsymbol{r}_j, \boldsymbol{r}_k)$ of electron pairs of the atomic system of interest are correlated only over distances $|\boldsymbol{r}_j-\boldsymbol{r}_k| \ll \hbar/q$. This condition is met by low density gases which are properly regarded as assemblies of small independent molecules but is not met by denser materials whose electrons are correlated over distances $>\hbar/q$. It was believed until the 1950's that, at least, molecular or ionic solids and liquids could be treated on the same basis as gases, but this model proved to be of uncertain applicability owing to the influence of electric interaction between densely packed molecules or ions in their excited states.

In the application of stopping power theory to condensed materials, one can still utilize formally the low-Q approximation formula 22 provided that the oscillator strengths be defined by the double-limit procedure[15]

$$f_n = \lim_{\boldsymbol{q}=0} \lim_{Z=\infty} E_n |F_n(\boldsymbol{q})|^2/Q \qquad 41.$$

The limit $Z=\infty$ means that one includes larger and larger groups of atoms in the atomic system of interest. The f_n so defined still obey the sum rule 33, $\Sigma_n f_n = 1$. The energy levels E_n to be entered, together with the f_n, in the definition (Eq. 34) of I also must be understood to pertain to the limit $Z=\infty$.

Thus, longitudinal excitations in condensed materials may be included in the theory of stopping power merely by a more careful definition of f_n, E_n, and I. This redefinition has little consequence as long as the value of I for a condensed material is obtained from stopping power experiments. On the other hand, the problem of determining I for a condensed material by working out the f_n and E_n of the aggregate from the properties of its constituent atoms or molecules is difficult and, in the main, unsolved. Nevertheless, substantial understanding of this problem has been achieved, and is helped by relating the spectral levels and intensities observed under different conditions to a single macroscopic parameter, namely, the dielectric constant $\epsilon(\omega)$ of the material of interest. This parameter serves also to connect the quantum theory of stopping power with the classical one.

It is convenient for this purpose to consider three alternative expressions of ϵ, namely

$$\epsilon(\omega) = 1 + \alpha_t(\omega) \qquad 42a.$$

$$1/\epsilon(\omega) = 1 - \alpha_l(\omega) \qquad 42b.$$

$$\epsilon(\omega) = \frac{1+\frac{2}{3}\alpha_m(\omega)}{1-\frac{1}{3}\alpha_m(\omega)}, \qquad \frac{\epsilon(\omega)-1}{\epsilon(\omega)+2} = \frac{1}{3}\alpha_m(\omega) \qquad 42c.$$

[15] The symbol Z indicates, in this article, the number of electrons in the system (atom, molecule, aggregate) under consideration. It coincides with the atomic number, its usual meaning, only when the "system" consists of a single atom.

The quantities α on the right-hand side are different types of polarizability which manifestly coincide in the limit $|\epsilon-1| = |\alpha_t| \ll 1$. This limit is realized: (*a*) for a low density gas at all frequencies ω, and (*b*) at very high frequencies for all materials.

In case (*b*), intra-atomic forces are negligible as compared to the electrons' inertia so that the material behaves as a free electron gas, for which

$$\alpha(\omega) = -4\pi e^2 NZ/m\omega^2 = -\omega_p^2/\omega^2 \qquad 43.$$

where NZ is the electron density and ω_p is called the plasma frequency. Note that

$$\hbar\omega_p = (4\pi\hbar^2 e^2 NZ/m)^{1/2} = 29[(\rho)_{g/cm^3} Z/A]^{1/2} \text{ eV} \qquad 43a.$$

where ρ is the density of the material and Z/A its number of electrons per unit atomic weight. In case (*a*) the polarizability is expressed in terms of the energy levels E_n of single molecules and of the corresponding oscillator strengths by the familiar expansion

$$\alpha(\omega) = \omega_p^2 \Sigma_n \frac{f_n}{E_n^2/\hbar^2 - \omega^2 - i\gamma\omega} \qquad 44.$$

where γ represents a very small damping constant. The essential effects of damping can be treated by considering, instead of Equation 44, its limiting form

$$\lim_{\gamma=0} \alpha(\omega) = \omega_p^2 \Sigma_n \frac{f_n}{E_n^2/\hbar^2 - \omega^2} + i\pi\omega_p^2 \Sigma_n f_n \delta(\omega^2 - E_n^2/\hbar^2) \qquad 44a.$$

In a condensed material, each of $\alpha_t(\omega)$, $\alpha_l(\omega)$, and $\alpha_m(\omega)$ possesses an expansion 44, but with different spectral parameters E_n and f_n, which are observed, as we shall see, under different conditions. The key point for us is that Equations 42a, b, and c establish a link between the different spectra. In particular, the function $\alpha(\omega)$ obtained by entering in Equation 44 the values of f_n defined by Equation 41 and the corresponding levels E_n of low-Q longitudinal excitation has been identified with $\alpha_l(\omega)$ [Fano (43), Sec. 5]. This set of levels and strengths is observed in the spectra of energy losses experienced by fast electrons traversing thin ($\sim$500 Å) films of material [see, e.g., Marton et al. (77)]. On the other hand, the f_n and E_n pertaining to the expansion of $\alpha_t(\omega)$ come under direct observation in the study of optical properties of a material, since $\epsilon(\omega) = 1+\alpha_t(\omega)$ is the square of the refractive index. Finally, the Lorentz-Lorenz formula 42c is relevant to gases and to cubic lattices of molecules; provided the short-range molecular interactions in these materials are not too strong, the spectral characteristics of $\alpha_m(\omega)$ remain close to those of single molecules.

A striking manifestation of the link between the spectra observed in different circumstances is found in metals and semiconductors. The strong optical absorption of these materials in the infrared implies that the expansion of $\alpha_t(\omega)$ involves a continuum of levels with large strengths f_n in this range. It follows then from Equation 44a that the real part of

$\epsilon(\omega) \doteq 1+\alpha_t(\omega)$ is large and negative in the visible and near ultraviolet, as shown by metallic reflection. No energy levels E_n of longitudinal excitation, which correspond according to Equation 44a to peaks in the imaginary part of $1/\epsilon(\omega) = 1-\alpha_l(\omega) = 1-\alpha_t/(1+\alpha_t)$, can then occur in this range. These levels occur instead at higher frequencies where $|\alpha_t|$ has decreased to the point where $\mathrm{Re}(1+\alpha_t)$ vanishes and metallic reflection subsides. A characteristic energy level of intense longitudinal excitation by charged particles traversing a metal is indeed observed near the energy where a metal stops reflecting. This energy may be regarded as one quantum $\hbar\omega_p'$ of free oscillation of the plasma of conduction electrons, where $\omega_p'^2 = 4\pi e^2 NZ'/m$ and NZ' is the density of electrons participating in the infrared optical absorption.

The upward shift of the main level of longitudinal excitation with respect to the levels of optical (transverse) excitation arises from the Coulomb repulsion of electrons over distances of the order of $\hbar/q$. Because of this strong interaction, the excitation involves a very large number of electrons and thus acquires a collective character which has been studied in some detail only for the model of free conduction electrons in metals [Bohm & Pines (22)]. The importance of the upward level shift for the stopping power of metals (where $\ln E_n$ would be $-\infty$ if the levels of the spectrum of α_t were relevant) was first appreciated by Kronig & Korringa (67), Kramers (66), and Bohr (23). A similar shift appears to occur, to a greater or smaller degree, in all condensed materials, but both theory [see, e.g., (1, 43, 44, 92)] and experimental evidence [see e.g. (77, 102)] are still fragmentary. Knowledge of $\epsilon(\omega)$, which embodies all spectral properties of long-wave excitations, throughout the range of interest into the far ultraviolet is quite scarce; and attempts at detailed verification of the consistency of longitudinal and transverse spectra, through Equations 42a and b, are just beginning [LaVilla & Mendlowitz (69)].

Our remaining task in this section is to express the energy loss of charged particles through longitudinal low-Q excitations in terms of $\epsilon(\omega)$. To this end one can multiply the right-hand side of the definition 34 of I by $2\int_0^\infty \omega d\omega\, \delta(\omega^2 - E_n^2/\hbar^2) = 1$ and rearrange the result by means of Equations 44a and 42b, to yield

$$\ln I = \frac{2}{\pi\omega_p^2}\int_0^\infty \omega d\omega\, \mathrm{Im}\left[\frac{-1}{\epsilon(\omega)}\right] \ln \hbar\omega \qquad 34a.$$

A similar adaptation of Equations 32 and 35 yields

$$N\Sigma_n E_n \int_{Q\min}^{Q_1} (d\sigma_n)_{\mathrm{longit.}} = \frac{2\pi z^2 e^4}{mv^2} NZ\Sigma_n f_n \ln\frac{2mv^2Q_1}{E_n^2}$$

$$= \frac{z^2e^2}{\pi v^2}\int_0^\infty \omega d\omega\, \mathrm{Im}\left[\frac{-1}{\epsilon(\omega)}\right] \ln\frac{2mv^2Q_1}{(\hbar\omega)^2} \qquad 45.$$

One also can obtain the same Equation 45 by macroscopic theory, considering the energy and momentum losses experienced by a charged particle as it traverses a medium characterized by $\epsilon(\omega)$ [Fröhlich & Pelzer (49), Hubbard (57)]. Notice, in Equations 34a and 45, that $\mathrm{Im}[-1/\epsilon(\omega)] = \mathrm{Im}[\epsilon(\omega)]/|\epsilon(\omega)|^2$;

thus the difference between the optical spectrum and that of longitudinal excitations is represented by the factor $1/|\epsilon(\omega)|^2$. This factor may be attributed to the dielectric screening of the squared electric field of the incident particle and reduces to 1 in the low density limit.

2.11 *Low-Q transverse excitations in condensed materials.*—The density of a material influences the nature of transverse excitations very substantially and, in particular, changes the trend of the stopping power versus energy curve in the high energy limit. This effect of strong interactions among atoms within the material may be described from different points of view. It was first studied by Fermi (45) and others [and reviewed by Uehling (130)] by treating the material as a macroscopic medium in which the field of an incident particle propagates and dissipates energy. Here we shall continue to utilize an atomistic point of view.

A main difference between longitudinal and transverse excitations lies in the occurrence, for transverse excitations of momentum q, of the energy cq which photons with this momentum have in empty space. Atomic electrons interact by emission and reabsorption of these photons not only with the incident particle but also with one another. This interaction is weak in a gas because of the small number of electrons perturbing each other; the derivation of the perturbation formula 12 may be said to assume that each excited state n of the material contains a small admixture of photon excitation. In condensed matter, perturbation theory no longer suffices to treat the coupling between electrons and photons. Neamtan (90) emphasized that the strength of this coupling is indicated by the departure from unity of the refractive index $n=[\epsilon(\omega)]^{1/2}$ which is proportional to the momentum-energy ratio for a photon.

In the presence of tight coupling, long-wave—i.e., low-q—transverse excitations are represented by superpositions of electronic excitations and of photons with comparable amplitudes. The properties of these excitations are represented in terms of the dielectric constant $\epsilon(\omega)$ of the material [Fano (43)]. Their energy levels $\hbar\omega$ are given by the roots ω of $c^2q^2-\omega^2\epsilon(\omega)=0$. The cross section for excitation of such a level, which corresponds to the second term of the atomic cross section (Eq. 25) multiplied by N, is

$$N\hbar\omega(d\sigma_\omega)_{\text{trans.}} = \frac{z^2e^2}{\pi v^2}\omega d\omega \,\mathrm{Im}\left[\frac{\beta^2\sin^2\psi}{1-\beta^2\epsilon(\omega)\cos^2\psi}\right]\frac{d(\cos^2\psi)}{\cos^2\psi}$$

$$= \frac{z^2e^2}{\pi v^2}\omega d\omega\beta^4\frac{\sin^2\psi\,\epsilon_2(\omega)}{[1-\beta^2\epsilon_1(\omega)\cos^2\psi]^2+\beta^4\epsilon_2^2(\omega)\cos^4\psi}d(\cos^2\psi) \qquad 46.$$

where $\epsilon_1=\mathrm{Re}\epsilon$, $\epsilon_2=\mathrm{Im}\epsilon$. Integration over $\cos^2\psi$ yields the analog of the second and third terms on the right-hand side of Equation 32

$$N\hbar\omega(d\sigma_\omega)_{\text{trans.}} = \frac{z^2e^2}{\pi v^2}\omega d\omega\,\mathrm{Im}\left\{\left[\beta^2-\frac{1}{\epsilon(\omega)}\right]\ln\frac{1}{1-\beta^2\epsilon(\omega)}\right\}$$

$$= \frac{z^2e^2}{\pi v^2}\omega d\omega\left\{\frac{\epsilon_2(\omega)}{|\epsilon(\omega)|^2}\ln\left[(1-\beta^2\epsilon_1)^2+\beta^4\epsilon_2^2\right]^{-1/2}\right.$$

$$\left.+\left[\beta^2-\frac{\epsilon_1(\omega)}{|\epsilon(\omega)|^2}\right]\arctan\frac{\beta^2\epsilon_2}{1-\beta^2\epsilon_1}\right\} \qquad 47.$$

In the low density limit ($\epsilon_2 \to 0$, $\epsilon_1 \to 1$), this formula reduces to the corresponding portion of (32).[16]

The logarithmic divergence of Equation 32 for $\beta \to 1$ stems from the fact that emission of a photon by a free incident particle is barely prevented by conservation of energy and momentum when β approaches 1 [Fano (42)]. When proper account is taken of the interaction between photons and atomic electrons, emission of radiation is seen to be possible indeed at frequencies for which $\epsilon_1(\omega) > 1/\beta^2 > 1$, more specifically, according to Equation 46, at $\cos^2 \psi = 1/\beta^2\epsilon(\omega) < 1$. This emission is the Cerenkov radiation which may be described as consisting of "dressed" photons, i.e., of photons accompanied by electron excitation; the coupling reduces the dressed photon's energy from cq to $cq(\epsilon_1)^{1/2}$. The integral over $\cos^2 \psi$ corresponding to this emission is now seen to be finite and to contribute the second term on the right-hand side of Equation 47, where the arctangent approaches π for $\beta^2\epsilon_1(\omega) > 1$.

The total energy loss through low-Q transverse excitations is obtained by integrating Equation 47 over ω from 0 to ∞. The integration succeeds best by complex variable techniques (45, 55, 118) summarized in App. B of (43). Its results are discussed in (130)[17] and have been represented by inserting in the braces of Equation 35 a "density effect correction" $-\delta$,[18] where

$$\delta = \frac{2}{\pi\omega_p^2}\left\{\int_0^\infty \omega d\omega \, \mathrm{Im}\left[\frac{-1}{\epsilon(\omega)}\right] \ln\left(1 + \frac{l^2}{\omega^2}\right) - \frac{\pi}{2} l^2(1-\beta^2)\right\}$$
$$= \Sigma_n f_n \ln\left(1 + \frac{\hbar^2 l^2}{E_n^2}\right) - l^2 \frac{1-\beta^2}{\omega_p^2} \qquad 48.$$

[16] The spectral distribution (Eq. 47) of transverse excitations produced by a charged particle differs from the distribution of excitations produced by incident white light because of different circumstances affecting the momentum transfer in the process.

[17] References (130, 55, 118, and 121) set out to treat simultaneously the effects of atomic interaction on longitudinal and transverse excitations. The oscillator strengths f_i and frequencies ν_i in these references pertain to isolated atoms or molecules; separate frequencies l_i are introduced which correspond to the E_n of the present treatment and are defined by $l_i = (\nu_i^2 + \omega_p^2 f_i)^{1/2}$ [Sternheimer (120)]. This relationship between the spectra of aggregates and of single atoms implies that $\hbar\omega_p f_n^{1/2} \ll |E_{n+1} - E_n|$, an assumption that would be inadequate to treat the spectra of optical electrons in condensed matter per se, but appears adequate for the calculation of δ. In fact, it is regarded as adequate to lump together into a single pair of parameters (f_i, l_i) the oscillator strengths and levels pertaining to the excitation of each atomic shell or subshell.

[18] Since δ modifies the contribution of low-Q transverse excitations in the braces in the middle of Eq. 38, namely $\ln[1/(1-\beta^2)] - \beta^2$, and since δ is in fact comparable to this contribution under all relevant conditions, one might cease treating δ separately as a "correction" and instead consider directly the correct contribution

$$\ln\frac{1}{1-\beta^2} - \beta^2 - \delta = \Sigma_n f_n \ln\frac{I^2}{(E_n^2 + \hbar^2 l^2)(1-\beta^2)} - \beta^2 + l^2\frac{1-\beta^2}{\omega_p^2}$$

This expression clearly reduces to $\ln[1/(1-\beta^2)] - \beta^2$ for $l^2 \ll (E_n, \hbar\omega_p)$ and to $2\ln(I/\hbar\omega_p)$ in the opposite limit $1-\beta^2 \ll 1$, $l^2(1-\beta^2) \to \omega_p^2$.

and l, an imaginary frequency, is the root of

$$1 - \beta^2\epsilon(il) = 0 \qquad 49.$$

that is,

$$\alpha_i(il) = \Sigma_n f_n \frac{\omega_p^2}{E_n^2/\hbar^2 + l^2} = 1 - \beta^2 \qquad 49a.$$

This root does not exist at low energies where $\beta < 1/\epsilon_1(0)$, in which case $\delta = 0$. As β^2 increases above $1/\epsilon_1(0)$ toward 1, l^2 increases from 0 towards infinity and eventually—at extremely high energies—it becomes proportional to $1/(1-\beta^2)$, so that the second term of Equation 47 equals unity and

$$\delta \to \ln \frac{\hbar^2\omega_p^2}{I^2(1-\beta^2)} - 1 \qquad 50.$$

Note that the f_n and E_n in Equations 48 and 49a pertain to the expansion of α_l, that is, are the same as appear in Equation 47. Note also that the density of electrons in the material has a determinant influence on the value of l, since ω_p^2 is proportional to NZ.

The numerical evaluation of l for any given material and value of β may appear difficult, because very little information is available on the function $\epsilon(\omega)$. However, this function behaves simply on the imaginary axis of ω, decreasing monotonically from $\epsilon(0)$ to 1 as shown by Equation 43. Therefore, crude information on the f_n and E_n suffices for an estimate of l. The most detailed studies and calculations of δ have been carried out by Sternheimer (118, 121)[17]; tabulations are described in Section 8.

2.12 *High-Q effects at extreme relativistic energies.*—The density effect removes the low-Q contribution to the $\ln[1/(1-\beta^2)]$ singularity of the stopping power formula 38, that is, one half of this singularity. The remaining part of the singularity, which arises from free recoil collisions with higher and higher Q, requires both reinterpretation and corrections at extremely high energies.

The probability, per unit track length, of collisions that produce recoils with energy in excess of any given large value E_n decreases almost as fast as E_n^{-1} for increasing E_n. Therefore, for sufficiently large E_n, the occurrence of such recoils becomes insignificant as compared to the occurrence of nuclear or bremsstrahlung processes. In other words, at extremely large incident energies, where very large E_n can in principle occur and contribute significantly to the stopping power (mean energy loss), the stopping power itself is no longer a relevant quantity because it is excessively influenced by unlikely extreme fluctuations. A relevant quantity is given in Section 7.1.

At extremely high energies of the incident particle, where condition 7 breaks down, corrections are required by the theory of stopping power. Some of these corrections allow for the failure of small recoil approximations like Equation 8, i.e., for the fact that the incident particle may lose an increas-

ingly large fraction of its energy in a single collision as E approaches and overtakes $(M/m)Mc^2$. Among these corrections is the replacement of the expression 20 of Q_{max} with 20a. Other corrections allow for the interaction between the spin of the incident particle and the atomic electrons. They are introduced as additional terms on the right of Equation 14, terms that depend on the spin and magnetic moment of the incident particle. Results based on simple assumptions on the magnetic moment for spin $\frac{1}{2}$ and 1 are given by Equations 3 and 4 of (130). Comparable results applicable to protons, with their anomalous moment, could be readily obtained but may never have been formulated as they would become important only for $E > 100$ GeV.

2.13 *Failures of the Born approximation and their correction.*—The basic cross-section formula 11 results from a calculation to the lowest non-vanishing order of approximation in the interaction between the incident particle and the atomic electrons. When the incident particle is much faster than the atomic electrons, Equation 16a can also be justified as the result of an impulse approximation, that is, as the product of the exact (Rutherford) cross section for collision with a free electron and of the probability that the elcctron recoil q yields an excitation of the atomic system to its level E_n. In the opposite limit, when the incident particle is much slower than the atomic electrons, its influence is much weaker than that of the nuclear charge, and the Born perturbation approach is also well justified[19] [see particularly the analysis by Henneberg (56)].

In the intermediate range of velocities, Equation 11 is not on firm foundations. Any error introduced by this equation has presumably been taken into account, together with others (shell corrections), through semiempirical procedures discussed in Section 4. Barkas points out, however (personal communication), that the next-higher-order correction to the Born approximation contributes to the stopping power in proportion to the cube of the incident particle's charge $(ze)^3$. Therefore, this correction is of opposite sign for negative and positive particle pairs, such as $\mu^{\pm}$, $\Sigma^{\pm}$, protons and antiprotons. It could thereby be separated from shell corrections at particle velocities comparable to those of inner electrons but still large enough to prevent the more obvious effect of electron capture by the positive particles. Indeed, evidence has been accumulating of a significant range excess of Σ^- over Σ^+ hyperons generated under comparable conditions. No evidence of comparable accuracy appears to exist for other particle pairs. The theory of this effect remains to be developed.

There are also radiative corrections to the basic theory which result from

[19] This statement applies, of course, only to incident heavy particles, whose motion remains nearly unperturbed, and not to electrons. For electron-atom collisions the Born approximation breaks down altogether unless the incident electron is much faster than the atomic electron.

the multiple virtual emission of photons by the incident particle. Recently, Tsytovich (129) has carried out a calculation of this effect to order e^4 and $e^4\ln^2(e^2)$. He emphasizes that the interaction of the virtual photons with the material magnifies the effect greatly for extremely high particle energy and high density of the material. The relevant condition is that the group velocity of virtual X-ray photons be smaller than the particle velocity. Tsytovich finds that the logarithmic factor in the "$e^4\ln^2(e^2)$" correction can become quite large so that the stopping power is reduced by 5–10 percent for densities $\sim$4 g/cm^3 and energies $E \gtrsim 200\ Mc^2$. Experimental evidence in agreement with this result has been presented [see Sec. 7.1 (93)].

3. The Mean Excitation Energy I

The mean excitation energy I, defined by Equation 34 or 34a (Sec. 2.10), is the main parameter of the stopping power formula 38. Its determination presents considerable difficulty because the most important excitation energies E_n lie in the range of 10 to 1000 eV where the oscillator strengths f_n are poorly known. On the other hand, I represents an average, and, further, only moderate accuracy of I itself is required for the determination of the stopping power, because an uncertainty ΔI causes a relative error on the stopping power approximately equal to $(\Delta I/I)/\ln(2mv^2/I)$, where the logarithm is of the order of 5 in the range of interest.

According to the Thomas-Fermi statistical model, atoms with different atomic numbers Z have spectral distributions of oscillator strengths, f_n versus E_n, with the same shape and differing only by a factor Z in the scale of frequencies ω or energy levels E_n.[20] Therefore, I itself is proportional to Z in the approximation of this model (17). Further considerations (Sec. 3.2) show the ratio I/Z to be approximately 10–15 eV and to be larger at lower than at higher Z. Beyond this fundamental information, provided by theory, the main reliance is placed on experimental data at this time.

The most significant data for this purpose have been obtained with protons of 300–700 MeV [Bakker & Segrè (3), Mather & Segrè (78), Zrelov & Stoletov (143), Barkas & von Friesen (6)], that is, in the energy range where the corrections C/Z and δ in expression 38 are hardly significant. Until very recently, these data appeared to be in disagreement with data obtained (36) from good measurements with 10–20 MeV protons. However, the values of the stopping power in medium and heavy elements at these lower energies are affected by substantial shell corrections. It has become progressively clear since 1958 [Brandt, Lindhard (85)] that these corrections had been underestimated (see Sec. 4) and that experimental results at the higher and lower energies are in fact consistent.

Table I presents a set of current estimates of I and of the ratio I/Z for

[20] Bloch (17) formulated the equation that governs this distribution, but the equation has apparently never been solved.

TABLE I

CURRENT ESTIMATES OF I[a]

	Substance	Z	I(eV)	I/Z	Reference (generally only latest published values cited)
H	atomic	1	15.0 (theor.)	15.0	(32)
	molecular		19 (theor.)	19	(96)
			18.3 ± 2.6		(76)
	in compounds		15–18		(128)
He		2	42 ± 3	21	(31)
			41.8 (theor.)		(82)
Li		3	40, 38	13	(23, 3)
			45, 38.8 (theor.)		(23, 37)
Be		4	64		(35)
			60, 66 (theor.)	16	(23, 37)
C	graphite	6	81	13.5	(128)
	in compounds		77–80		(128)
N	molecular	7	88	12.6	(128)
	in compounds		79–102		(128)
O	molecular	8	101		(128)
	in compounds		91–101	12.6	(128)
Al		13	163	12.6	(13)
Ar		18	190	10.6	(31, 76)
Fe		26	273	10.5	(143)
Cu		29	315	10.9	(143, 6)
Kr		36	360	10.0	(14)
Ag		47	471[b]	10.0	
Au		79	761[b]	9.6	
Pb		82	788[b]	9.6	(6)
U		92	872[b]	9.5	(6)
Emulsion		—	323	—	(6)
Air		—	85	—	(89)
CH_4		—	45	—	(31)

[a] In some cases values have been renormalized to $I_{Al} = 163$ eV or $I_{Cu} = 315$ eV.

[b] These values have been lowered to take into account the fact that shell corrections, as represented by C/Z in Equation 38, do not vanish at $v \to c$ (cf. Sec. 4.4). In the case of Pb, for example, the nonvanishing of C/Z is equivalent to a lowering of I by approximately 32 eV; in the case of Ag, 7 eV.

a number of elements.[21] Interpolation in Z should be dependable to a few per cent of the value of I in the range $Z > 20$ in which the great majority of atomic electrons belongs to closed shells, because the properties of closed

[21] In previous literature, I was determined by fitting Eq. 38 to stopping power data at high energy with the assumption that the shell correction C/Z vanishes in

shells are smooth functions of Z. Notice that I/Z decreases fairly regularly as Z increases, except for low Z. The high values of I/Z at low Z can be attributed to the "extra-stiffness" that results from the tighter binding of valence electrons as compared to the prediction of the Thomas-Fermi model. A slow decrease of I/Z throughout the periodic system results from exchange effects, which also stiffen the atoms but matter less and less as Z increases and the repulsion and exchange among inner shell electrons fade out as compared to nuclear attraction. A modified Thomas-Fermi treatment that includes exchange effects [Jensen (58), Brandt (29, 85)] leads to $I/Z = a + bZ^{-2/3}$ where a and b are constants, difficult to estimate dependably.

The information in Table I and in the preceding paragraph is incomplete and tentative in many respects. A more complete survey may be found in *NBS Handbook 79* (89). Even though the accuracy on the value of I for heavy metals now attains a few percent, the same cannot be said for other materials. For example, the same value $I = 190$ eV has been found for argon in two good experiments (31, 76), but its error range is stated to be ± 17 eV; on the other hand, interpolation on I/Z between aluminum and copper leads one to expect $I \sim 216$ eV for argon. A "low" value reported for neon (89) has been found to be erroneous (87). Thus one should not conclude that the I/Z values for the noble gases are systematically lower than for metals, and that this outer shell effect is felt very strongly for Z as high as 18 and appreciably for $Z = 36$ (Kr); note that one might have predicted the opposite effect on the basis of outer shell binding energies. This and other uncertainties make additional experimentation, particularly with Thompson's arrangement (128), desirable, especially now that the connection between measurements at high and low energies has been clarified.

3.1 *Chemical combination and aggregation effects.*—A material containing a density N_i of various elements of atomic number Z_i can be treated in first approximation, according to Bragg's additivity rule, as a combination of atoms which contribute separately to its stopping power. Equation 38 is then adapted to this material by setting in it

$$NZ = \Sigma_i N_i Z_i, \qquad NZ \ln I = \Sigma_i N_i Z_i \ln I_i \qquad 51.$$

An effective value of I is thereby defined for the material as a logarithmic average over the I_i for its constituent atoms, in keeping with Equation 34.

This approach proves remarkably accurate even though it disregards

the high energy limit. The data of Table I take into account that C/Z does not vanish in this limit because it depends on the velocity ratio of the atomic electrons and the incident particle. This ratio remains larger than zero and is not always very small because the incident particle's velocity does not exceed c. The difference between these points of view is barely significant at the current level of accuracy, because C/Z modifies the stopping power by less than 1 percent at high energies and I by a few percent at most (see Sec. 4, Eqs. 58 and 59).

chemical bonds and other aggregation properties of the material, which modify the stopping power through changes of the spectrum of excited levels E_n and through the density effect (Secs. 2.10 and 2.11). Several circumstances contribute to this accuracy, namely:

(*a*) Chemical bonds and other aggregation properties influence almost exclusively the contribution of valence electrons to the stopping power,[22] whereas this contribution constitutes a small fraction of the total for all but the lightest elements. Experimentally, an influence of chemical structure on stopping power, of the order of 1 percent, has been clearly demonstrated by Thompson (128) for light elements traversed by high energy protons.

(*b*) Valence electrons with particularly low binding in an isolated atom, which give a small contribution to the atomic I_i, are generally very active chemically and tend to form compounds with strong heteropolar bonds and higher contribution to I_i. Thus chemical binding in the common and stable substances tends to smooth out the variations of spectral levels and oscillator strengths of valence electrons along the periodic system. The effective I of a compound tends to be a smooth function of the logarithmically averaged Z of its constituent elements. Therefore application of Equation 51 with interpolated values of I_i (rather than realistic values applicable to isolated atoms) may yield a rather realistic value for the effective I.

(*c*) The electric interaction between distant particles in condensed matter, discussed in Section 2.10, also raises the spectral levels E_n of valence electrons just in those substances, like metals, where E_n would otherwise be particularly low. Here again aggregation has the effect of smoothing out the variations of f_n and E_n for valence electrons as functions of Z_i.

Some systematic effects of the chemical state of aggregation are nevertheless present. The presence of unsaturated bonds, which possess low-lying excitation levels, reduces I as shown by Thompson's comparison of the stopping powers of aromatic and aliphatic hydrocarbons (128). Alkali metals, with a single valence electron and low density, have a particularly low I inasmuch as the main E_n of the valence electrons lies at 5.3 eV for sodium as compared to 15 eV for aluminum.

An important example of a complex physicochemical system is photographic emulsion, where the track length of particles serves as a measure of their energies. Range-energy relations and other track properties in emulsions have been studied by many authors (130, p. 338), particularly in recent years by Barkas and his co-workers (4). The value of I determined by fitting the stopping power formula 38 to the observed range in Ilford G 5 emulsion has been reported to be 328 eV (6), whereas the corresponding value calculated by entering in expression 51 the known composition of this

[22] Inner shell electrons contribute very little to the zero-frequency dielectric constant, and their contribution to the density effect can accordingly be ignored except at extreme relativistic energies of incidence, as shown by Eqs. 49a and 48.

emulsion[23] and the values of I_i for the individual elements from Table I is 300 eV (4). It is not clear how this discrepancy should be solved.

3.2 *Calculations of* I.—Direct calculation of I has been carried out thus far only for a few light substances after sufficient information had been gathered on their spectral distribution of oscillator strengths f_n. The results are: H (atomic), 15.0 eV (10, 32); H_2 (gas), 19 eV (96, 100); He, 41.8 eV (82) or 41.5 eV (38); CH_4 (gas), 42.8 (100). Crude, but perhaps adequate, estimates of f for numerous substances might be feasible at this time; additional experimental and theoretical information on this subject will probably come forth in the next several years.

An interpolation method which relates I to other properties of the electronic ground state of atomic systems has been proposed by Dalgarno (37). The mean values $\langle E^r \rangle = \Sigma_n f_n E_n{}^r$ for various integers r between -8 and 2 can be obtained from observable optical properties or calculated from ground-state wave functions. If r is now regarded as a continuous variable, we have, owing to Equation 34,

$$\ln I = [d\langle E^r \rangle / dr]_{r=0} \qquad 52.$$

Applications of this procedure (37) yield $I = 14.8$ eV for H, 41.7 for He, 38.8 for Li, and 66.1 for Be.

Attempts at estimating the spectral properties of valence electrons from experimental polarizability data [Westermark (136), Brandt (28, 30)] appear unpromising inasmuch as they imply an estimation of the slope at $r = 0$ in Equation 52 from a knowledge of only the two ordinates at $r = -2$ (polarizability) and at $r = 0$ (sum rule 33).

Lindhard & Scharff (72) introduced an approach that emphasizes the approximate correspondence between the excitation levels E_n and the various atomic shells. They associate a characteristic frequency to each volume element of the atom, which depends on the local electron density as the plasma frequency does in a free-electron gas. Thereby a functional correspondence is established between the optical absorption spectrum $f(\omega)$ of an atom or molecule and the density distribution $\rho(r)$ of its electrons, with $\omega = [\chi 4\pi e^2 \rho(r)/m]^{1/2}$ and χ a proportionality constant of the order of 1 or 2. Information on the density $\rho(r)$ derived from Hartree-model calculations or from other models can then be utilized to calculate, in accordance with Equation 34, $\ln I = Z^{-1} \int dr\, \rho(r) \ln[\hbar\omega(r)]$. Results of remarkable accuracy are obtained. Brandt (30) has exploited this approach further. The tentative nature of the initial assumptions should, however, be borne in mind when dealing with detailed applications of the Lindhard-Scharff procedure.

Systematic studies of the small departures from Bragg's rule (Eq. 51) for different chemical combinations of elements would be interesting, but the

[23] In units of 10^{20} atoms/cm^3: $N_{Ag} = 101.01$, $N_{Br} = 100.41$, $N_I = 0.565$, $N_C = 138.30$, $N_N = 31.68$, $N_S = 1.353$, $N_H = 321.56$, $N_O = 94.97$.

Thompson experimental results (128) do not provide adequate guidance. An effort to extend Thompson's work would also be of interest as a problem of chemical physics. Brandt's extensive efforts in this direction (28, 30) rest on uncertain assumptions as indicated above.

4. Inner Shell Corrections

The stopping power theory, as presented in Section 2, rests on the assumption that the speed of the incident particle is much higher than that of the atomic electrons in their normal bound states. In fact, this approximation is often poor. Significant corrections are required at all energies in heavy elements, and substantial departures from the results of Section 2 occur in all but the lightest elements for protons below 100 MeV. As the velocity of the incident particle decreases, the full line in Figure 2, which limits the range of integration, moves up and leftward so as to wipe out the "empty crescent," which characterizes the all-important intermediate-Q range of approximation.

Even before this approximation breaks down altogether, corrections are required to carry the low-Q approximation of Section 2.5 beyond the first significant term and to improve the high-Q approximation of Section 2.7 in the range of $Q \sim Q_{max}$. Notice that the cutoff of the integration in Equation 37 at $Q = Q_{max}$ excludes incorrectly the region of integration indicated with horizontal hatching in Figure 3 and includes spuriously the region with vertical hatching. These two errors compensate each other to a large extent but their net effect vanishes only in the limit considered in Section 2.7, where the shaded area becomes infinitely narrow.

An example of directly observable collisions with E_n and Q larger than Q_{max} is afforded by the ejection of K electrons of medium and heavy elements by protons of a few MeV [Merzbacher & Lewis (80)]. For example, the cross section for ejection of K electrons in nickel by protons has a peak value of approximately 10^{-21} cm^2 near 20 MeV, at which energy Q_{max} is 5 times the minimum E_n for this process; a 10-fold reduction in proton energy, which brings Q_{max} well below the minimum E_n, reduces the cross section by only a factor of 10. [At still lower energies the cross section should eventually decrease as E^5 according to Henneberg's theory (56), but departures from this law have been observed by Messelt (81).]

As mentioned in Section 2.8, the departures from the results of that section due to insufficient velocity of the incident particle are represented by the corrective term C/Z in Equation 38.[24] Partial success has been obtained in estimating this term by a variety of empirical and theoretical approaches. Among the factors that influence the value of C/Z we shall not consider any

[24] Roughly speaking, one may say that the electrons of the inner shells, K, L, . . . cease to contribute to the stopping power in succession as the incident particle's velocity decreases. However, the cutoff of each shell is gradual.

effects of relativity on the motion of the atomic electrons or of the incident particle or any inaccuracies in the treatment of the effects of the transverse interaction. Thus, in the theoretical approach we shall regard C/Z as defined[25] in terms of the function

$$L(v, Z) = \ln \frac{2mv^2}{I} - \frac{C}{Z} = \tfrac{1}{2}\Sigma_n E_n \int_{E_n^2/2mv^2}^{\infty} |F_n(q)|^2 \frac{dQ}{Q^2} \qquad 53.$$

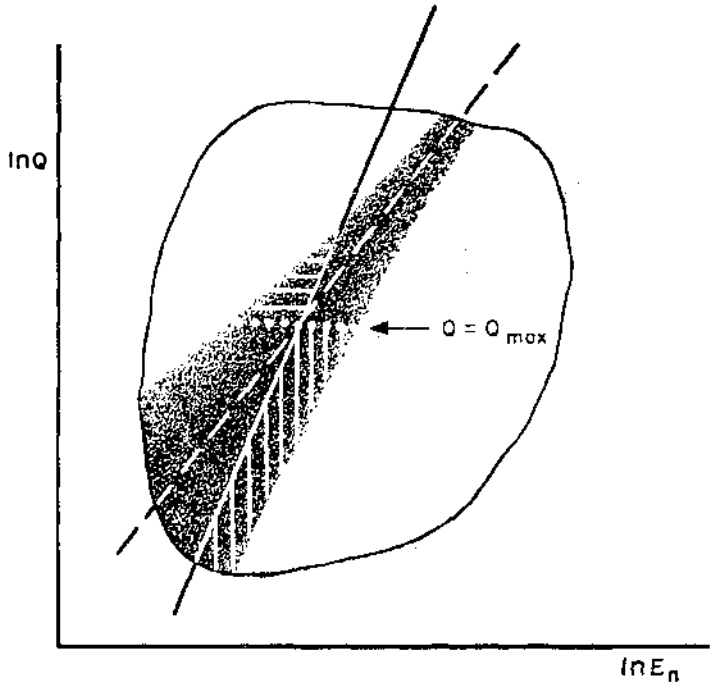

FIG. 3. Detail of Fig. 2 showing the region around Q_{max} for moderate velocity of incidence.

However, in the empirical approaches L or C/Z will be chosen by fitting Equation 38 to experimental results, i.e., by setting

$$L(v, Z) = \ln \frac{2mv^2}{I} - \frac{C}{Z} = \frac{mv^2}{4\pi r^2 e^4 NZ}\left(-\frac{dE}{ds}\right)_{exper.} - \ln \frac{1}{1-\beta^2} + \beta^2 + \tfrac{1}{2}\delta \qquad 53a.$$

[25] The correction C/Z is defined here as an average over the contributions of the several shells, with $C = C_K + C_L + \cdots$, where C_K, C_L are commonly used in the literature (130, 134). This interconnection requires the factor $\frac{1}{2}$ to appear on the right-hand side of 53.

regardless of the physical significance that is thereby attributed to L.[26]

The theoretical *nonrelativistic* definition of C/Z implied by Equation 53 can be cast into a form convenient for further analysis [Walske (134)]. To this end, we introduce the symbol $f_n(Q) = E_n|F_n(q)|^2/Q$—such that $f_n(0)$ coincides with the optical oscillator strength f_n—and recall the following facts from Section 2: (*a*) Equation 27 implies $\Sigma_n f_n(Q) = 1$ irrespective of Q; (*b*) $\ln(2mv^2/I)$ represents in effect $\frac{1}{2}\Sigma_n \int_{I^2/2mv^2}^{2mv^2} f_n(Q)dQ/Q$; (*c*) the integral $\Sigma_n \int_0^{I^2/2mv^2} [f_n(Q) - f_n(0)]dQ/Q$ vanishes because of (*a*) above; (*d*) the definition of I, Equation 34, is such that

$$\Sigma_n \int_{E_n^2/2mv^2}^{I^2/2mv^2} f_n(0)dQ/dQ = 0.$$

Thereby, Equation 53 is seen to be equivalent to

$$\frac{C}{Z} = \tfrac{1}{2}\Sigma_n \int_0^{En^2/2mv^2} [f_n(Q) - f_n(0)] \frac{dQ}{Q} - \int_{2mv^2}^{\infty} f_n(Q) \frac{dQ}{Q} \qquad 53b.$$

This expression has been evaluated numerically for atomic H by Walske (134)†; the result is shown in Figure 4 for purposes of orientation. The scale of abscissas, $\ln x = \ln(v/v_0)^2$, where $v_0 = c/137$ is the root mean square velocity of the electron in H, has been chosen so that the curve approaches the straight line

$$y = \ln(2mv^2/I) = \ln x + 1.29 \qquad 54.$$

at large x, where C/Z becomes negligible. Notice that the curve fails to depart much from the straight line except at excessively low energies even though the conditions that would lead to Equation 38 with $C/Z = 0$ fail completely at $x < 1$. For this reason C/Z is called a "correction" even though its definition by means of expression 53 abandons the method of Section 2.5–2.8 altogether. The initial drop of $L(v, Z = 1)$ below the straight line Equation 54, as v decreases, indicates reduced ability of the incident particle to excite the atomic electron; the tail of the curve toward low v indicates that some ability persists even after v has fallen below v_0.

[26] In setting up Eq. 38 one has dumped, by implication, into C/Z the influence of all inaccuracies of the theory of Sec. 2, because the other corrective term δ is fully defined by Eq. 48. To proceed consistently with the spirit of note 12, one should define C/Z firmly by means of Eq. 53 and insert a new corrective term $\mathfrak{C}$ in Eq. 38 to represent all other effects. This procedure appears premature because we have no adequate basis at present for estimating C and $\mathfrak{C}$ separately. (See, however, the comment in Sec. 2.13 on the stopping power for particles of negative charge.)

† However, the coefficient 19/6 in Equation 11, p. 1287 of *Phys. Rev.*, 88 (1952) is incorrect; its value is 25/6, namely, the same as that of the corresponding coefficient in the companion Equation 13.

4.1 *Calculations with hydrogenic wave functions.*—Because the innermost electrons are fastest, they might be expected to have a dominant influence on C/Z at higher energies of the incident particle.[27] Because their motion is controlled primarily by the nuclear attraction, their contribution to $L(v, Z)$

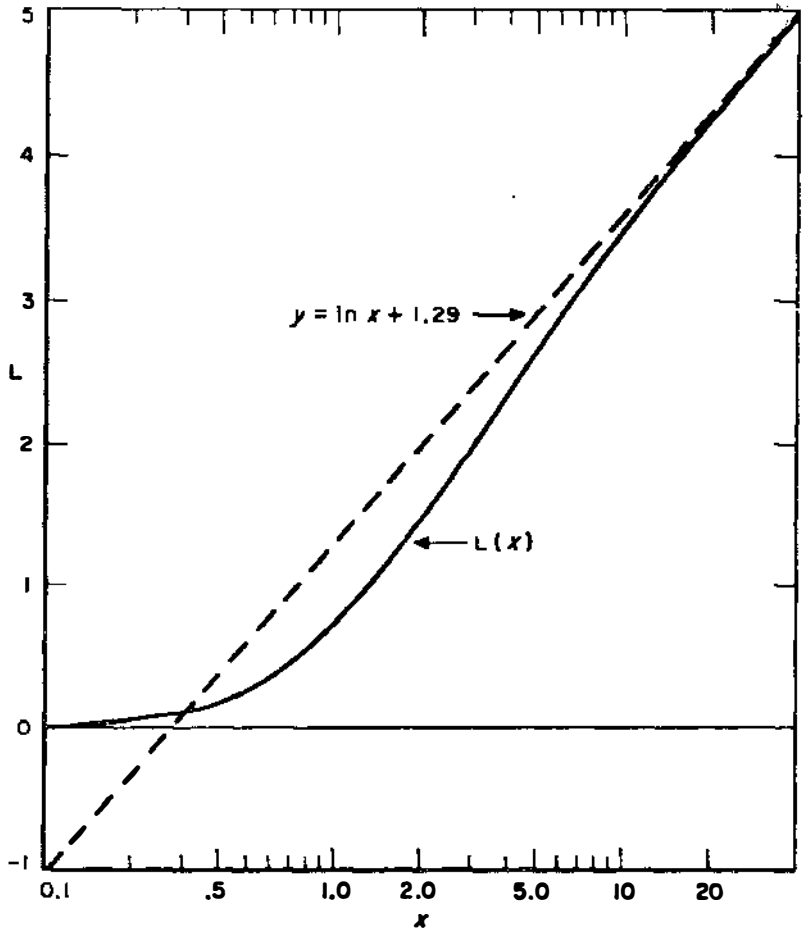

FIG. 4. L for atomic hydrogen as a function of $x=v^2/v_0^2=E_{\text{keV}}/25$. (Courtesy J. E. Turner.)

may be calculated rather accurately by evaluating $F_n(q)$ with hydrogenic wave functions, with screening adjustments that make them applicable to all elements. Laborious calculations by this method have been carried out for K and L electrons (73, 134). Their results have been reviewed by Uehling

[27] This expectation is not really borne out, as shown in Sec. 4.4 below.

(130). These and analogous calculations account approximately for the probability of ejection of K and L electrons by protons of a few MeV (80, 81). Extension of this method to M electrons has been regarded as prohibitively laborious. On the other hand, M electrons are now known to contribute greatly to C/Z below 100 MeV in most materials (see Fig. 6).

4.2 *The statistical model.*—As noted in Section 3, the ratio I/Z should be the same for all atoms according to the Thomas-Fermi model. It may, then, be convenient to represent $\ln(2mv^2/I)$ in Equation 53 as $\ln(v^2/Zv_0^2) + \ln(2mv_0^2Z/I)$, where $\ln(2mv_0^2Z/I) \sim 1.7$ is roughly equal for all materials and $v^2/v_0^2Z = x$ is the same as x in Equation 54 for $Z=1$. It was argued by Lindhard & Scharff (72) that the whole right-hand side of Equation 53 should depend on v and Z only in the combination v^2/Z, within the accuracy of the Thomas-Fermi model.[28] Accordingly, $L(v, Z)$ should be represented by a single curve for all elements when plotted against x as in Figure 4. In fact, Reference (72) defines L as $L(x)$.

Figure 5 shows that experimental estimates of L for different elements fall within a single strip when plotted against x, so that this type of plot proves useful. On the other hand, one cannot draw a single line that represents all results within much better than 10 percent. No better fit should have been expected in view of the variations of I/Z noted in Section 3.

By the procedure indicated on p. 28, Lindhard & Scharff (72) obtained an approximate theoretical evaluation of the entire curve $L(x)$. Their result has the same trend as the bundle of curves in Figure 5. In particular, for $x < 5$, a good agreement was found between experimental results and the theoretical expression $L(x) = 1.36x^{1/2}$.

4.3 *Extended application of hydrogenic calculations.*—In view of the difficulty of extending the calculations of Section 4.1 to the M and higher shells, Bichsel (14) has assumed that C_M, namely, the contribution of M electrons to C, depends on the particle's velocity in the same way as the C_L contribution calculated by Walske (134),[29] except for the scale factors. The same assumption was made for further shells. The scale factors were then determined, separately for the various M, $N \cdots$ subshells, by simultaneous least square fitting of Equation 38 to a large number of experimental stopping power and range data on each of various elements. The results appear reasonable in that, after the fitting, the contribution of each subshell is found to depend primarily on the ratio of the particle velocity to the root mean square velocity of the electrons in that subshell.

[28] More specifically, it is argued on p. 8 of (72) that $L(v, Z)$ should depend only on the ratio of $Q_{max} = 2mv^2$ to the characteristic frequencies of the Thomas-Fermi atom which are proportional to Z. Notice, however, that L might also depend on the ratio of Q_{max} to the mean kinetic energy $\langle K \rangle_0$, which determines the width of the shaded strip in Fig. 2 and which is proportional to $Z^{4/3}$. An indication of relevance of $v^2/Z^{4/3}$ appears in Sec. 4.4.

[29] Notice, however, that the plots of the K- and L-shell contributions differ in shape somewhat.

The numerical work required by this approach is rather extensive in view of the limited accuracy and dependability of the data and procedures that are involved and tends to obscure the link between input and output. Nevertheless, this method has proved valuable for the purposes of correlating a large mass of data and of producing extensive numerical tables of stopping power (see Secs. 4.5 and 8).

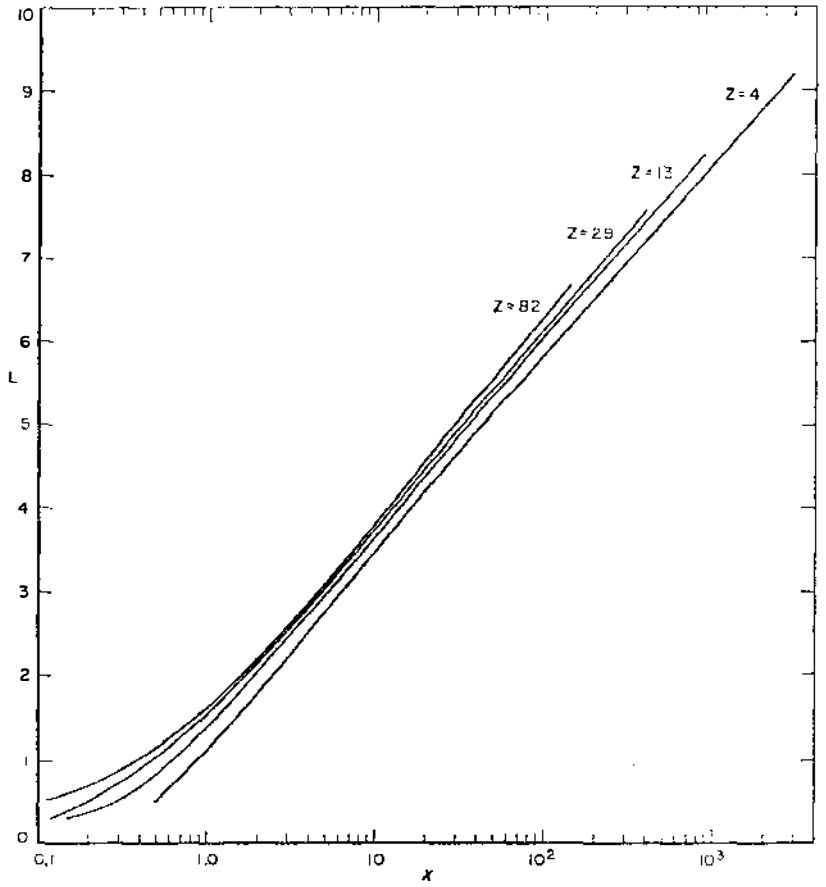

FIG. 5. L for various metals as a function of $x = v^2/v_0^2 Z$. (Courtesy J. E. Turner.)

4.4 *Expansion in powers of* $1/v^2$. Because the shell correction vanishes in the limit where the incident particle is infinitely faster than the atomic electrons, its behavior near this limit is studied appropriately by expanding the expression 53b into inverse powers of the incident particle's velocity. This study was initiated by Brown (32) and developed by Walske (134) for

atomic H and hydrogenlike atomic electrons and is being extended to other atoms by Fano & Turner (87). Analogous results on the stopping power of an electron gas emerge from recent work by Lindhard & Winther.* The significance of these developments remains limited by their nonrelativistic character.

Walske (134) pointed out that the Σ_n in the expression 53b is conveniently split into two parts corresponding, respectively, to energy transfers smaller and larger than $\sim mv^2$, the exact point of separation being irrelevant for calculations to order $(1/v^2)^2$. The values of the two partial sums will be called C_1 and C_2, respectively. The contribution to C_1 of the second integral in 53b arises from the region of Figure 2 with $Q > 2mv^2$, $E_n < mv^2$, which is unshaded; in fact this contribution is of order $(1/v^2)^5$ and will be disregarded here. The contribution to C_2 of the term with $f_n(0)$ consists only of canceling that of the term with $f_n(Q)$ at low Q and can be disregarded, to order $(1/v^2)^2$, if the integrations over Q are simultaneously limited to the range $mv^2 \lesssim Q \lesssim 4mv^2$ in the calculation of C_2.

To calculate C_1, one expands the remaining integrand[30]

$$f_n(Q) - f_n(0) = \Sigma_{r=1} \frac{1}{r!} \left(\frac{d^r f_n}{dQ^r}\right)_{Q=0} Q^r \qquad 55.$$

and then integrates over Q term by term. This yields

$$\frac{C_1}{Z} = \tfrac{1}{2}\Sigma_n{}^{(1)} \Sigma_{r=1} \frac{1}{r!r} \left(\frac{d^r f_n}{dQ^r}\right)_{Q=0} \left(\frac{E_n^2}{2mv^2}\right)^r \qquad 56.$$

The operations $\Sigma_n{}^{(1)}$ and $\Sigma_r (d^r/dQ^r)_{Q=0}$ can now be carried out in reverse order, so that C_1 is expressed in terms of the sums over states

$$\Sigma_n{}^{(1)} E_n{}^{2r} f_n(Q) = \Sigma_n{}^{(1)} E_n{}^{2r+1} \left| F_n(q) \right|^2 / Q \qquad 57.$$

Expressions such as 57 are evaluated by closure when the sum extends over a complete set of states. Thereby one obtains sum rules which express the sum in terms of the mean values of certain physical quantities (e.g., the electron kinetic energy) over the ground state of the atom.[31] In the present application $\Sigma_n{}^{(1)}$ excludes the states of highest excitation energy. This exclusion is of no consequence for $r = 1$ or 2, because in this case the states of highest excitation would contribute negligibly to $[(d/dQ)^r \Sigma_n E_n{}^{2r} f_n(Q)]_{Q=0}$; we replace then $\Sigma_n{}^{(1)}$ with Σ_n for $r = 1, 2$. For $r > 2$, the states of highest excitation contribute so heavily that the Σ_n would diverge whereas $\Sigma_n{}^{(1)}$ is finite; therefore, sum rules cannot be utilized to calculate $\Sigma_n{}^{(1)}$.

* Thanks are due to Prof. J. Lindhard for information on his unpublished work and for calling the author's attention to certain essential points.

[30] This expansion need not cause concern in itself, because F_n depends on q through an exponential whose convergence is assured.

[31] This procedure is similar to that used by Placzek (95) on neutron scattering.

Since, on the other hand, the separation of the contributions C_1 and C_2 is of practical relevance only up to expansion terms of order $(1/v^2)^2$, we limit the present treatment to the order of approximation $r \leq 2$ and set

$$\frac{C_1}{Z} \sim \frac{K_1}{2mv^2} + \frac{K_2}{(2mv^2)^2} \qquad 58.$$

where the coefficients are found, by sum rules, to be

$$K_1 = m\langle v^2\rangle_0 + \text{correlation terms} \qquad 58a.$$

$$K_2 = m^2\langle v^4\rangle_0 + \frac{10\pi}{3}\frac{\hbar^2e^2}{m}\langle\rho(0)\rangle_0 + \text{correlation terms} \qquad 58b.$$

In these formulas $\langle v^2\rangle_0$ and $\langle v^4\rangle_0$ are the mean squared and mean fourth-power velocity of an atomic electron in the ground state of the atom, averaged over all electron shells, and $\langle\rho(0)\rangle_0$ is the mean electron density at the center of the atom. The "correlation terms," which depend on statistical pair-correlations of electrons, would vanish in the Hartree model and presumably yield a correction smaller than 10 percent; these terms will be disregarded here and treated further in (87).

Utilizing a current estimate (52) of the total binding energy of electrons (which is related to their kinetic energy by the virial theorem), we find

$$\frac{K_1}{2mv^2} \sim \frac{mv_0^2Z^{1.4}}{2mv^2} \approx \frac{Z^{0.4}}{2x} \qquad 59a.$$

The Thomas-Fermi model yields $Z^{1/3}$ instead of $Z^{0.4}$ on the right-hand side of 59a.[28] In an independent electron approximation one can assess the contribution of the various inner shells to K_1, and one finds them approximately equal.[32] With regard to K_2, to which K electrons contribute most, $\langle v^4\rangle_0$ and $\langle\rho(0)\rangle_0$ have been estimated crudely by hydrogenic nonrelativistic wave functions. This yields

$$\frac{K_2}{(2mv^2)^2} \sim \frac{bZ^3(2mv_0^2)^2}{(2mv^2)^2} + \frac{10\pi}{3}\frac{\hbar^2e^2}{m(2mv^2)^2}\frac{Z^3}{\pi a^3}2.4 \sim \frac{b+2.0}{x^2}Z \qquad 59b.$$

where b is a number of the order of 2 or 3 which increases slowly with Z. This result indicates that the second term of Equation 58 amounts to about 1/2 of the first one for protons of 700 MeV in uranium, and that this ratio is far smaller for lighter elements. On the other hand, the second term's importance increases rapidly as the proton energy decreases.

With regard to the evaluation of C_2/Z, the following situation exists at this time. Walske's calculation of C_2/Z for atomic H in its ground state, to

[32] If unscreened hydrogenic wave functions were used, the $\langle v^2\rangle$ of each electron would be proportional to the inverse square of its principal quantum number, n^{-2}, a factor which is exactly balanced by the existence of $2n^2$ electrons in a complete shell. Screening makes the binding energy of successive shells decrease faster than n^{-2}, but it also makes $\langle mv^2/2\rangle$ larger than the binding energy, in accordance with the modification of the virial theorem for a nonhydrogenic field; these two effects of screening cancel out approximately.

order $(1/v^2)^2$, yields exactly the same result as the corresponding calculation of C_1/Z (corrected as indicated in note† on p. 31); the same holds for his calculation of C_2/Z for atomic H in its $n=2$ state, which was carried out to order $1/v^2$ only (134). The same result, $C_2=C_1$ to order $(1/v^2)^2$, is again reported by Lindhard and Winther* for an electron gas. The discovery of this result for quite different systems suggests that it may have general validity. Accordingly, despite the absence of conclusive evidence on this point we proceed, in Section 4.5, on the *assumption* that $C_1=C_2$, i.e.,

$$\frac{C}{Z}\sim 2\left[\frac{K_1}{2mv^2}+\frac{K_2}{(2mv^2)^2}\right] \qquad \text{to order } \left(\frac{1}{v^2}\right)^2 \qquad 58c.$$

Notice that Equation 58 constitutes an expansion in inverse powers of the particle velocity rather than of its energy. Therefore, in the high energy limit, the shell correction C/Z approaches a nonzero value, corresponding to $v=c$, rather than zero. This result is implicit in the fact that Equation 53 depends on $v=dE/dp$ rather than on E, and is also borne out by the hydrogenic calculations (134).

4.5 *Summary of evidence.*—The experimental and theoretical evidence on shell corrections is represented conveniently either by a plot, analogous to Fig. 4, of $L(v, Z)$ versus $\ln x=\ln(v^2/v_0^2Z)$ (Fig. 5) or by plotting the departure of L from a straight line, namely, $C/Z=\ln x-L(v, Z)+\ln(2mv_0^2Z/I)$, also against $\ln x$ (Fig. 6). The "experimental" values of L are, of course, obtained from Equation 53a.

Figure 5 shows that L has for all elements the same general shape as that shown for atomic hydrogen in Figure 4, but departs from a straight line even less than in the case of hydrogen. The decrease in value of I/Z with increasing Z is reflected in the fact that the L curves lie above one another in order of increasing Z for large x, where C/Z becomes negligible. (Exceptions to this rule are expected for low-Z elements.) As x decreases, C/Z increases at first for all elements, as shown by Equations 58 and 59, but more rapidly for higher-Z ones, so that the L curves tend to draw nearer to one another. Figure 6 shows the same data in the more traditional form of shell correction curves. The sum of the theoretical K- and L-shell contributions for copper and lead, according to Walske (134), is indicated for purposes of orientation.

Because the curves for different elements do not lie far apart from one another and presumably do vary smoothly with Z for $Z>10$, it appears possible to estimate from Figure 5 or, better, from Figure 6 the value of L for each v and Z to within a very few percent.

Figures 5 and 6 may be described as an extract of experimental evidence on proton stopping power obtained by Bichsel (14) (see Sec. 4c) and by Whaling (137) at very low energies. If available results of individual measurements of stopping power for different elements were entered as points in the

* Thanks are due Professor J. Lindhard for information on his unpublished work and for calling the author's attention to certain essential points.

graphs, as in Figure 1 of (72), they would disperse over the region traversed by the curves and exhibit to visual inspection little systematic trend as functions of the atomic number. Each curve in the figures results, instead, from prior smoothing and interpolation of the data for one element. The elements chosen belong to a set of metals which have been studied extensively and whose atomic numbers span almost the whole periodic system.

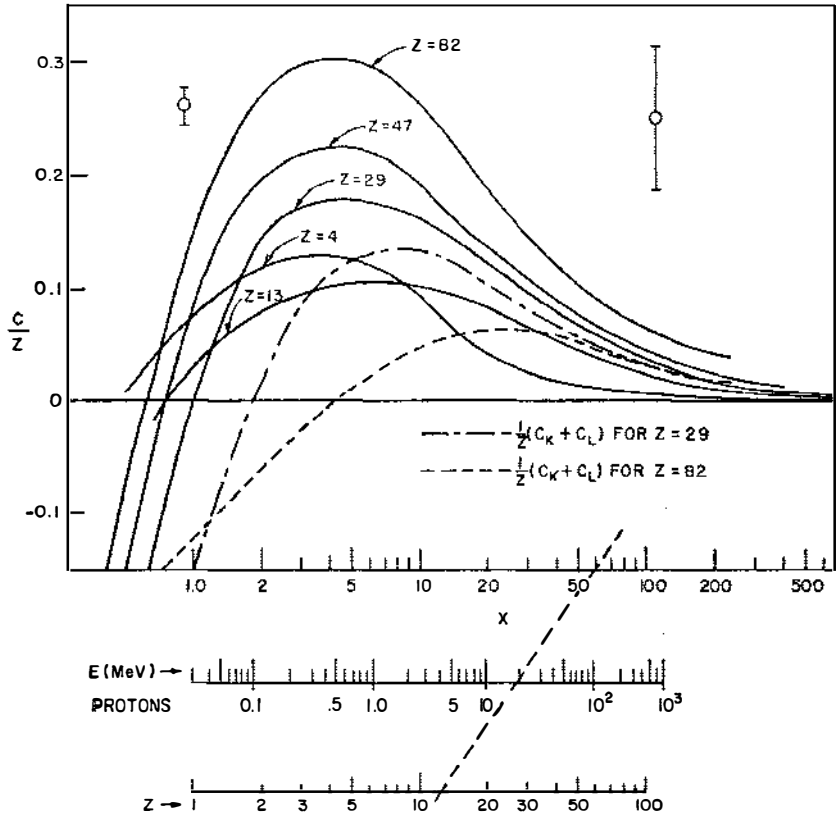

FIG. 6. C/Z for various metals as a function of $x = v^2/v_0^2 Z$. The error bars represent the approximate effect of 1 per cent error in the stopping power at the respective abscissas for all elements. The example of nomogram use shows that $x = 59$ for 20 MeV protons in aluminum. (Courtesy J. E. Turner.)

More specifically, the curves have been drawn through points taken from Bichsel's and Whaling's stopping power tables. Bichsel's tables, in turn, were obtained from a form of Equation 38 in which C/Z is represented as a specified function of the particle energy and of a number of free parameters.

These parameters, as well as the excitation energy I, were then adjusted to attain a best fit of Equations 38 and 39 to a large selection of stopping power and range data pertaining to each element under consideration. Bichsel states that a fit was obtained throughout to 1 percent or to the experimenter's estimate of his error, whichever is larger.

A small departure from Bichsel's results was introduced in Figures 5 and 6 at high energies, to allow for the fact that C/Z does not vanish at $\beta=1$ as assumed by Bichsel. Estimates of C/Z at $\beta=1$ were obtained from Equations 58 and 59, and each curve of Figure 6 was moved up or down to terminate at the correct value for $\beta=1$ (i.e. for $x=137^2/Z$). A corresponding correction was thereby made on I. These corrections are barley significant.

For purposes of orientation, some error bars corresponding to a ± 1 percent variation of the stopping power—roughly, the order of accuracy of the present state of the art—are shown in Figure 6. In view of the magnitude of this uncertainty in comparison to the rather small values of C/Z, only the major trends of the curves can be regarded as significant.

Despite this low level of significance and despite the lack of a direct recheck of the fitting to experimental data, independent of Bichsel's procedure, the curves in Figures 5 and 6 may afford a basis for a systematic study of C/Z throughout the periodic system. They show a rather clear, systematic, and plausible trend as functions of Z. They permit at least a tentative interpolation to obtain the value of C/Z or L for each material and each particle velocity. Incidentally, they also show, in comparison with the sample results of Walske (134), how unpromising the approach was through a theoretical shell-by-shell calculation of C/Z.

5. Energy Straggling

Statistical fluctuations of the number and kind of collisions along the track of a particle cause the effect of "straggling," i.e., of unequal energy loss along the tracks of particles that travel under identical conditions. Because of this effect, different particles starting under identical conditions have tracks of different lengths, and the range formulas of Section 2.9 represent only a mean value of these lengths; the formulas also require some correction indicated in Section 5.3.

Three closely related distributions result from straggling, namely: (*a*) the energy distribution

$$f(E, s)dE \qquad 60a.$$

of particles that have traveled a pathlength s under identical initial conditions; (*b*) the pathlength distribution

$$\frac{f(E, s)ds}{\int_0^\infty f(E, s)ds} \qquad 60b.$$

of particles whose energy has been reduced from an initial value E_0 to a given value E; (c) the distribution

$$\left[-\frac{d}{ds}\int_E^{E_0} f(E', s)dE'\right] ds \qquad 60c.$$

of the pathlength traveled by particles up to the collision at which their energy drops below the value E. Note that (b) and (c) differ because the energy of a particle drops in jumps and does not lie in turn at every level between E_0 and 0. [For additional discussion of these distributions, see Fano (40).] The distribution of total pathlength ("range straggling"), which is considered most frequently, is the limit of expression 60c for $E \to 0$. The distribution function $f(E, s)$ obeys the equation

$$\frac{\partial f(E, s)}{\partial s} = -N\Sigma_n\sigma_n(E)f(E, s) + N\Sigma_n\sigma_n(E + E_n)f(E + E_n, s) + \delta(E - E_0)\delta(s) \qquad 61.$$

where the last term represents the production of the particle at $s=0$ with the source energy E_0.

The normalization integral in Equation 60b is of interest, because

$$y(E)dE = \left[\int_0^{\infty} f(E, s)ds\right] dE \qquad 62.$$

represents the mean value of the pathlength traveled by each particle while its energy lies between $E+dE$ and E in the course of its slowing down. This quantity serves to calculate the yield of reactions produced by a particle during its slowing down. For example, if protons penetrate a material containing $\mathfrak{N}$ nuclei per cm^3 with a cross section $\sigma(E-E_{res})$ for a (p, γ) resonance reaction, the reaction yield per proton is $\mathfrak{N}\int_0^{E_0} \sigma(E-E_{res})y(E)dE$. The differential pathlength $y(E)$ obeys the equation

$$N\Sigma_n\sigma_n(E)y(E) = N\Sigma_n\sigma_n(E + E_n)y(E + E_n) + \delta(E - E_0) \qquad 63.$$

which can be solved numerically (113). In the approximation that disregards straggling and was utilized in the range formulas of Section 2.9, one takes

$$y(E) \sim [N\Sigma_n E_n\sigma_n(E)]^{-1} = (-dE/ds)^{-1} \qquad 64.$$

This result follows from Equation 63 by expanding $\sigma_n(E+E_n)$ $y(E+E_n)$to first order in E_n and integrating over E.

As a heavy particle loses all or most of its energy, it experiences a great number of collisions in which all classes, including the less frequent ones with larger energy losses, are well represented. Therefore extreme fluctuations are quite unlikely over a long pathlength, and the straggling distributions are very nearly Gaussian. This result hinges on the circumstance that the maximum energy loss Q_{max} amounts normally to a very small fraction, $\sim 4m/M$, of the total energy of a heavy particle. The straggling distributions are far from being Gaussian when Q_{max} is comparatively large, i.e.: when condition 7 is violated at extremely high energies (Sec. 2.12), or when

one deals with short sections of path over which the energy loss is not much larger than $Q_{\max}$, or for incident electrons under any condition.

As an index of the importance of unlikely fluctuations over a short pathlength s, one may consider the energy loss ξ' which is exceeded once, on the average, i.e., such that $Ns\Sigma_n^{(E_n>\xi')}\sigma_n = 1$. Under conditions of high-Q approximation (Sec. 2.7) we have

$$\xi' = \frac{2\pi z^2 e^4}{mv^2} NZs \left(1 - \frac{\xi'}{Q_{\max}} - \xi' \frac{1-\beta^2}{mc^2} \ln \frac{Q_{\max}}{\xi'}\right) \tag{65.}$$

Large fluctuations are prominent when $\xi' \ll Q_{\max}$. The energy ξ' thus defined cannot exceed $Q_{\max}$. It has been found convenient to consider, instead of ξ', the energy

$$\xi = \frac{2\pi z^2 e^4}{mv^2} NZs \tag{65a.}$$

which coincides with ξ' when $\xi' \ll Q_{\max}$ but becomes $\gg Q_{\max}$ when large fluctuations are unimportant. The numerical value of ξ is

$$(\xi)_{\text{kev}} = \frac{0.154}{\beta^2} z^2 \frac{Z}{A} (s)_{\text{mg/cm}^2} \tag{65b.}$$

Thus we have two main situations of interest, namely, that of long pathlengths, with $\xi/Q_{\max} \gg 1$ and Gaussian fluctuations, and that of short pathlengths, with $\xi/Q_{\max} < 1$ and prominent large fluctuations. In both cases simplifications arise from the fact that the collision cross sections vary by a negligible amount from one collision to the next, because $Q_{\max}$ is a small fraction of a heavy particle's energy. This derives in turn from the smallness of m/M, so that theoretical treatments rely in fact on expansions into powers of m/M.

5.1 *Long pathlengths; Gaussian straggling.*—This approximation is obtained by solving Equation 61 with $f(E+E_n, s)$ expanded into powers of E_n up to the second power only and with $\sigma_n(E+E_n) \sim \sigma_n(E)$. It is convenient to replace the pathlength s with the mean energy $\langle E \rangle$, which is related to s by[33]

$$s = \int_{\langle E \rangle}^{E_0} \frac{dE}{(-dE/ds)} \tag{66.}$$

This procedure yields

$$f(E, \langle E \rangle) = [2\pi \langle \Delta E^2 \rangle]^{-1/2} \exp\left[-\frac{(E - \langle E \rangle)^2}{2\langle \Delta E^2 \rangle}\right] \tag{67.}$$

where the mean square deviation $\langle \Delta E^2 \rangle$ results, according to Bohr (24), from the accumulated contributions of successive collisions

$$\langle \Delta E^2 \rangle = N \int_0^s \Sigma_n E_n^2 \sigma_n ds = \int_{\langle E \rangle}^{E_0} \frac{N\Sigma_n E_n^2 \sigma_n}{-dE/ds} dE = \int_{\langle E \rangle}^{E_0} \frac{\Sigma_n E_n^2 \sigma_n}{\Sigma_n E_n \sigma_n} dE \tag{68.}$$

[33] Notice that 66 coincides with the range formula Eq. 39 for $\langle E \rangle = 0$, $s = R$.

The calculation of $N\Sigma_n E_n^2\sigma_n$ proceeds analogously to that of the stopping power $N\Sigma_n E_n\sigma_n$ in Section 2. The basic sum rule 27 is replaced by

$$\Sigma_n E_n^2 \mid F_n(q) \mid^2 = Q^2 + \frac{4}{3} Q\langle K\rangle_0 + \text{correlation terms} \qquad 69.$$

where $\langle K\rangle_0$ indicates the mean kinetic energy of an atomic electron in the ground state of the atom, averaged over all electron shells, and where the "correlation terms"[34] are presumed to yield a correction smaller than 10 per cent. The low-Q limit of Equation 69, analogous to Equation 33, is

$$\Sigma_n E_n f_n = \frac{4}{3}\frac{1}{Z}\frac{\langle \mid \Sigma_i \mathbf{p}_i \mid^2\rangle_0}{2m} = \frac{2}{3} m \left\langle \frac{\mid \Sigma_i \mathbf{v}_i \mid^2}{Z} \right\rangle_0 \qquad 70.$$

inclusive of correlation terms. The analog of Equation 24 defines a mean excitation energy I_1 weighted differently from I, namely,

$$\ln I_1 = \Sigma_n E_n f_n \ln E_n / \Sigma_n E_n f_n \qquad 71.$$

The result is

$$N\Sigma_n E_n^2\sigma_n \sim 4\pi z^2 e^4 NZ \left\{ \frac{1 - \beta^2/2}{1-\beta^2} + \frac{2}{3}\frac{\langle \mid \Sigma_i \mathbf{v}_i \mid^2\rangle_0}{Zv^2} \ln \frac{2mv^2}{I_1} \right\} \qquad 72.$$

The $\sim$ sign in this formula indicates that approximations have been made and corrective terms analogous to C/Z omitted. Relativistic corrections to the second term in the braces have been dropped because the second term is much smaller than the first one except when $\beta \ll 1$. In fact, the second term was disregarded altogether in Bohr's initial theory (24). Effects analogous to those represented by the shell correction C/Z to the stopping power formula do not appear to have been studied yet. Sternheimer (123) has carried out recently a rather accurate numerical evaluation of expression 72, including a modification to allow for the value (Eq. 20a) of $Q_{\max}$ at extremely high energies, where condition 7 breaks down.[35]

The pathlength distributions 60b and 60c, which coincide in the Gaussian approximation, are not conveniently obtained from Equation 67 where the pathlength s is represented indirectly by $\langle E\rangle$. Instead, one may return to solve Equation 61 in the same approximation used above, but replacing E with the mean pathlength $\langle s\rangle$ instead of replacing s with $\langle E\rangle$; the relationship of E and $\langle s\rangle$ is, however, the same as the relationship 66 of $\langle E\rangle$ and s. One finds, then,

$$f(\langle s\rangle, s) = [2\pi\langle \Delta s^2\rangle]^{-1/2} \exp\left[-\frac{(s - \langle s\rangle)^2}{2\langle \Delta s^2\rangle} \right] \qquad 73.$$

[34] The expression including electron correlations is

$$\Sigma_n E_n^2 \mid F_n(q) \mid^2 = \frac{Q}{2mZ} \left\langle \left| \sum_{j=1}^{Z} [\hat{q}\cdot\mathbf{p}_j \exp(iq\cdot r_j/\hbar) + \exp(iq\cdot r_j/\hbar)\hat{q}\cdot\mathbf{p}_j] \right|^2 \right\rangle_0$$

[35] Other effects mentioned in Sec. 2.12 also occur at these energies.

where (24)

$$\langle \Delta s^2 \rangle = \int_E^{E_0} \frac{N\Sigma_n E_n^2 \sigma_n}{(-dE/ds)^3}\, dE \qquad 74.$$

For the numerical calculation of $\langle \Delta s^2 \rangle$, which utilizes Equation 72, see (123).

5.2 *Short pathlengths; Landau-type approximations.*—When Equation 61 has to be integrated over a short interval of s, the expansion of $f(E+E_n, s)$ into powers of E_n cannot be utilized, because the spectrum of f is sharply peaked owing to the $\delta(E-E_0)$ factor in the source term. On the other hand, one can regard the cross sections $\sigma_n(E)$ and $\sigma_n(E+E_n)$ as equal to $\sigma_n(E_0)$ throughout the relevant range of integration. With this assumption, a Laplace transformation is applied conveniently by multiplying both sides of Equation 61 by $\exp[-p(E_0-E)]$ and integrating over E. Integration over s is then elementary and yields

$$\int_0^{E_0} dE \exp[-p(E_0-E)] f(E,s) = \exp\{-Ns\Sigma_n\sigma_n(E_0)[1-\exp(-pE_n)]\} \qquad 75.$$

Similarly one finds

$$\int_0^{E_0} dE \exp[-p(E_0-E)] y(E) = \{N\Sigma_n\sigma_n(E_0)[1-\exp(-pE_n)]\}^{-1} \qquad 76.$$

The problem resolves now into two separate parts: evaluation of the Σ_n and inversion of the transform, i.e., determination of $f(E, s)$ or $y(E)$ from a knowledge of the right-hand side of Equation 75 or 76.[36]

The calculation of the Σ_n in Equation 75 may begin by term-by-term summation over the expansion

$$1-\exp(-pE_n) = pE_n - (1/2)p^2E_n^2 + (1/6)p^3E_n^3 + \cdots.$$

The sum over the linear term is proportional to the stopping power and that over the second term is proportional to Equation 72. Since higher terms are weighted more heavily in favor of large E_n and, therefore, of large Q, they may be evaluted by means of the large-Q approximation 31 to σ_n. Use of this approximation yields an exponential integral without further resort to term-by-term summation. The result,

$$\begin{aligned} &Ns\Sigma_n\sigma_n(E)[1-\exp(-pE_n)] \\ &= p\xi\left\{\ln\frac{2mv^2}{\epsilon pI^2} + \ln\frac{1}{1-\beta^2} - \beta^2 - 2\frac{C}{Z} - \delta - \left(1+\frac{\beta^2}{pQ_{max}}\right)\int_{pQ_{max}}^{\infty} dt\,\frac{e^{-t}}{t}\right. \\ &\left. - \frac{1-\exp(-pQ_{max}) + \beta^2\ln(\gamma pQ_{max})}{pQ_{max}} - \frac{1}{3}pm\left\langle\frac{|\Sigma_j v_j|^2}{Z}\right\rangle_0 \ln\frac{2mv^2}{I_1}\right\} \end{aligned} \qquad 77.$$

with $\gamma = \exp C = 1.78107$ and $\epsilon = \gamma/e = \exp(C-1) = 0.6552$, has been given

[36] The inversion of the transform may be avoided for the purpose of experimental tests, since experimental data on $f(E, s)$ or $y(E)$ may be utilized to calculate the left-hand side of Eq. 75 or 76 numerically and compare the results directly with the right-hand side.

by Vavilov (133) except for the last term in the braces. This term, which is often small, corresponds to the last term of Equation 72 and to the Blunck-Leisegang (19) correction. Notice that the first five terms in the braces correspond to a stopping power formula from which the contribution of high-Q collisions with $Q > 1/p\epsilon$ has been eliminated. This group of terms was contained, in essence, in Landau's original theory (68), which regarded Q_{max} as infinitely large and thereby omitted the sixth and seventh terms. More accurately, the Landau result represents the limit of Equation 77 for $\xi/Q_{max} \ll 1$, with omission of the Blunck-Leisegang term.

Landau (68) first studied the inversion of the Laplace transform 75, within the approximation $\xi/Q_{max} \ll 1$ which yields

$$f(E, s) = \xi^{-1}F(\lambda) = (\xi 2\pi i)^{-1}\int_{-i\infty}^{i\infty} \exp(p\lambda + p \ln p)dp \qquad 78.$$

Here F is Landau's universal function of the single variable

$$\lambda(E, s) = \frac{E_0 - E}{\xi} - \left[\ln\frac{2mv^2\xi}{\epsilon I^2(1-\beta^2)} - \beta^2 - 2\frac{C}{Z} - \delta\right] \qquad 79.$$

which depends on s through ξ, and the path of integration in Equation 78 passes on the positive side of $p = 0$. The Landau function F peaks at $\lambda = 0.225$, drops off sharply on the negative side, and exhibits a λ^{-2} tail on the positive side. Numerical approximation methods that apply to intermediate values of ξ/Q_{max}, up to the large values of this ratio which yield a Gaussian curve, were developed by Symon (126) and described by Rossi (105). Vavilov (133) has also worked through the intermediate range quite successfully, obtaining $f(E, s)$ as function of λ and ξ/Q_{max}. He has shown that expansion of 77 into powers of p up to p^3 is adequate for $\xi/Q_{max} > 1$, in which case $f(E, s)$ is obtained analytically in terms of Airey's function (133, Eq. 13). Numerical curves obtained for $\xi/Q_{max} < 1$ reduce to the Landau curve at $\xi/Q_{max} \sim 0.01$. The remaining Blunck-Leisegang term in Equation 77, which was disregarded by Vavilov, can be taken into account as follows. If the energy distribution function calculated by Vavilov's method is called $\bar{f}(E, s)$, the corrected distribution is given by

$$(E, s) = \int_{-\infty}^{\infty} \frac{dE'}{\sqrt{\pi}\,\eta} \exp\left[-\frac{(E - E')^2}{\eta^2}\right] \bar{f}(E', s) \qquad 80.$$

where

$$\eta^2 = \frac{4}{3}\xi m\left\langle \frac{|\Sigma_i v_i|^2}{Z}\right\rangle_0 \ln\frac{2mv^2}{I_1} \qquad 80a.$$

A rapidly converging expansion for the differential pathlength $y(E)dE$ has been obtained from its transform 66 by Spencer & Fano (113), with the Landau approximation to Equation 77,

$$y(E) = \left[\frac{2\pi z^2 e^4 NZ}{mv^2}\right]^{-1}\left\{\frac{1}{\pi}\arctan\frac{\pi}{B} + \frac{\Gamma'(1)}{\pi^2 + B^2} + \frac{B\Gamma''(1)}{(\pi^2 + B^2)^2} + \cdots\right\} \qquad 81.$$

where the primes indicate derivatives of the gamma function and

$$B = \ln \frac{2mv^2(E_0 - E)}{\epsilon I^2(1 - \beta^2)} - \beta^2 - 2\frac{C}{Z} - \delta \qquad 81a.$$

For $B \gg \pi$, Equation 81 approaches the reciprocal stopping power formula 64, modified by removal of the contribution of collisions with $Q > (E_0 - E)/\epsilon$. For values of $E_0 - E \ll Q_{max}$, the quantity 81 becomes substantially larger than 64, showing that a particle travels an excess pathlength at the beginning of its penetration as though it had a small effective stopping power. This transient phase of penetration lasts until the particle has traveled a pathlength sufficient to render likely the occurrence of the less frequent larger energy losses. Once these losses have come into statistical equilibrium with the more numerous smaller ones, their full contribution to stopping power becomes effective and $y(E)$ drops to its normal value. The excess value of $y(E)$ at the beginning of penetration has been demonstrated by Walters et al. (135) as an excess yield of a (p, γ) resonance reaction when protons hit a target with an energy barely above the resonance.

5.3 *Corrections to long pathlength formulas.*—The range formula 39, the differential pathlength formula 64, and the Gaussian straggling formulas 67 and 73 involve errors of the order of $4m/M$ even for long pathlengths. Equation 64, which underlies the range formula, is derived under the assumptions that the cross sections σ_n for successive collisions differ negligibly from one another. Small variations of the cross section are taken into account by an expansion procedure (40) that replaces Equation 64 by

$$y(E) = \left(-\frac{dE}{ds}\right)^{-1} \left\{1 - \frac{1}{2}\frac{d}{dE}\frac{\Sigma_n E_n^2 \sigma_n(E)}{\Sigma_n E_n \sigma_n(E)} + \cdots\right\} \qquad 82.$$

(Localized sharp variations of $\sigma_n(E)$, if any, would give rise to transient disturbances of $y(E)$, akin to those represented by Equation 81 which stem from the sharpness of the initial energy spectrum.)

The correction in Equation 82 represents the fact that an unusually large energy loss exposes a particle to an unusually increased probability of further collisions. This effect reduces the total range, which is the integral of $y(E)$. However, it is overbalanced by the increase of $y(E)$ at the beginning of penetration which is large, even though limited to a narrow energy interval, as shown by Equation 81. There results a total net *increase* of the particle range which amounts to $\sim$1 percent for μ mesons. This increase was emphasized and calculated by Lewis (71) and discussed further by Fano (40).

Distortions of the Gaussian shape of straggling distributions may be expressed as departures of the various moments of the distributions, such as $\langle (E - \langle E \rangle)^n \rangle$, from the ratios prescribed by the Gaussian law. Each moment can be obtained, like $\langle \Delta E^2 \rangle$ in Equation 68, by summing the contributions of fluctuations in successive energy intervals. The gradual change of cross

sections introduces corrections to these contributions which are represented by perturbation formulas akin to Equation 82. For details of these calculations see (40) and (63). Lewis (71) has also given formulas that represent the distortion of the Gaussian range distribution corresponding to the corrected moments.

6. Multiple Scattering Effects on Penetration

The path of a heavy particle that penetrates a material is not quite straight. Therefore, the path's projection along its initial direction, i.e., the depth of penetration z, is a little shorter than the corresponding pathlength s. This difference is often of the order of 1 percent. It must accordingly be considered when data on the range (i.e., total pathlength) are obtained from observations of the thickness of material that is penetrated.

Determination of this correction requires a knowledge of the statistical distribution of $s-z$. A knowledge of the distribution of the angle θ between the path's directions at s and at $s=0$ is required for this purpose, since $dz=ds\cos\theta$ and[37]

$$\frac{d(s-z)}{ds} = 1-\cos\theta \sim \tfrac{1}{2}\theta^2 \qquad 83.$$

The distribution in θ is also involved rather subtly in the analysis of penetration experiments, e.g., when the particles are detected by a flat ionization chamber whose response depends on the obliquity of traversal.

In principle, the fluctuations in energy (i.e., the straggling discussed in Sec. 5), in $s-z$, and in θ are related and are governed by a single equation. This equation has been considered but only partial aspects of it have been solved. In practice, for heavy particles the correlations between fluctuations of different variables are rather small. For example, the fluctuations in θ at the end of the range depend primarily on collisions in the last sections of the path, whereas fluctuations in $s-z$ have been building up in comparable amounts all along the path.

The mean value of $s-z$ is found by taking the mean of Equation 83 at each value of the pathlength s and integrating

$$\langle s-z\rangle_s = \int_0^s \langle 1-\cos\theta\rangle_{s'} ds' \sim \int_E^{E_0} \frac{\langle 1-\cos\theta\rangle_{E'}}{-dE'/ds'} dE' \qquad 84.$$

The mean value $\langle 1-\cos\theta\rangle_s$ is obtained with rather good accuracy from the theory of multiple elastic scattering (9, 70, 107). Sample data on $\langle s-z\rangle/s$ are given in Table II (see p. 48). The ratio

$$v = 2\frac{s-z}{\langle s-z\rangle_s} \qquad 85.$$

is a natural variable for the distribution function of $s-z$.

[37] The small-angle approximation indicated on the right of Eq. 83 has been generally utilized for simplicity in studies of heavy-particle penetration. However, calculation of moments or other parameters of the distribution of $1-\cos\theta$ is actually more direct, is no more complicated, and avoids convergence difficulties.

Some useful qualitative remarks and approximate formulas for $\langle s-z \rangle$ are available. Recasting Equation 84 in the form

$$\langle s - z \rangle_s = \int_0^s \frac{d\langle 1 - \cos\theta \rangle_{s'}}{ds'} (s - s')ds' \qquad 84a.$$

shows that scattering at s', which is represented by $d\langle 1-\cos\theta\rangle_{s'}/ds'$, contributes to $\langle s-z\rangle_s$ in proportion to the remaining pathlength $s-s'$. [Similarly, the contribution of this scattering to higher moments $\langle (s-z)^n \rangle$ is proportional to $(s-s')^n$.] For this reason, scattering in the early portion of a track contributes appreciably to $\langle s-z\rangle_s$ even though it is weaker on account of the higher particle energy.

As seen from Equation 84, $\langle s-z\rangle$ is a function of the material and of the particle energy, which depends on the ratio of scattering to stopping power. Blanchard (15) emphasized that this ratio can be split into a material-dependent factor and an energy-dependent factor with greater accuracy than either the scattering or the stopping cross section alone. One finds for heavy particles

$$\langle 1 - \cos\theta \rangle_s \sim kZ \frac{m}{M} \ln \frac{E_0(E + 2Mc^2)}{E(E_0 + 2Mc^2)} \qquad 86.$$

where E_0 and E are the particle's kinetic energies at $s=0$ and at s, and k is a coefficient with a minor residual dependence on both material and energy, of which some values are given in Table II.[38] The material-dependent factor Zm/M results from the ratio of corresponding factors in the scattering and stopping power formulas. From Equation 86 follows

$$\langle s - z \rangle_s \sim Z \frac{m}{M} \langle l \rangle s \qquad 87.$$

where $\langle l \rangle$ is the approximate mean value of k times the logarithm in Equation 86 and lies generally between 0.3 and 0.6. Mather & Segrè (78) used, in essence, this formula with $k=1/2$ and with $\langle l \rangle = 0.28$ for Cu.[39] Considerations analogous to those presented here have led Barkas (7) to a scaling procedure that relates the value of $\langle s-z\rangle$ in a material of interest to the value for photographic emulsions which can be measured.

Because the distribution of $s-z$ is very skew, one may wish to single out a value of $s-z$ nearer to the peak of the distribution than the mean. Bichsel & Uehling (13) achieved this end, in effect, by entering in Equation 84 a typical value of $1-\cos\theta$, for each s', somewhat lower than the mean

[38] The proton values of k differ systematically from the value for electrons, $k=0.3$, given by Blanchard (15). Note that Eq. 86 is the first term of an exponential series in powers of m/M, which would converge poorly for electrons.

[39] An early, often utilized, treatment by E. J. Williams leads to the nonrelativistic form of Eq. 86, with $(E+2Mc^2)/(E_0+2Mc^2)=1$, and to $k=\frac{1}{2}$. Further application of the approximate range-energy formula $R=aE_0^b$ yields then the mean value $1/b$ for the logarithm in Eq. 86 and thereby $\langle l \rangle = k/b$ in Eq. 87.

TABLE II

(Courtesy M. J. Berger)

MEAN SCATTERING CORRECTION ON PROTON PENETRATION

$100\langle s-z\rangle_{s=R}/R$

Figures in parentheses are values of $\langle l\rangle$ in Equation 87

Proton initial energy (MeV)	Be, $Z=4$ $I=64$ eV	Al, $Z=13$ I=163 eV	Cu, $Z=29$ $I=314$ eV	Sn, $Z=50$ $I=516$ eV	Pb, $Z=82$ $I=826$ eV
1000	0.070 (0.32)	0.247 (0.35)	0.580 (0.37)	1.04 (0.38)	1.75 (0.39)
500	0.075 (0.34)	0.266 (0.38)	0.628 (0.40)	1.13 (0.41)	1.90 (0.43)
200	0.081 (0.37)	0.288 (0.41)	0.683 (0.43)	1.23 (0.45)	2.09 (0.47)
100	0.085 (0.39)	0.306 (0.43)	0.724 (0.46)	1.32 (0.48)	2.25 (0.50)
50	0.090 (0.41)	0.327 (0.46)	0.779 (0.49)	1.41 (0.52)	2.44 (0.55)
20	0.096 (0.44)	0.347 (0.49)	0.831 (0.53)	1.51 (0.55)	2.62 (0.59)
		Values of k in Equation 86			
1000	0.65	0.67	0.70	0.72	0.74
100	0.70	0.76	0.80	0.83	0.85
10	0.86	0.94	0.99	1.03	1.08

$\langle 1-\cos\theta\rangle_{s'}$. The result of the integration, which they called ΔR_0 and tabulated for a set of initial energies and materials, represents the value of $s-z$ for a "smoothed out path" which has a specified typical obliquity θ at each pathlength s'. The lack of smoothness of actual paths was then taken into account by increasing ΔR_0 by 2/15.

Yang (139) developed a rather detailed theory of the distribution function of $s-z$, applicable to short pathlengths over which the cross sections are regarded as constant and utilizing a diffusion approximation to multiple scattering. This theory shows that the distribution function vanishes rapidly as v approaches zero, with a dominant factor $\exp(-1/v)$, that it peaks at $v\sim 1$, and that it decreases for large v according to $\exp(-\pi^2 v/16)$.

For longer pathlengths, over which the cross sections vary substantially, moments of the distribution of $s-z$ can be calculated by a procedure introduced by Lewis (70). Studies by Spencer (114, 115), using this method as well as a theoretical analysis of the distribution for very small v, show that the $\exp(-1/v)$ law remains applicable. This result is also borne out by extensive Monte Carlo calculations which have provided much of the current information on the distribution of $s-z$ near the end of heavy-particle ranges [Berger (9, 87, 88)].

This recent study by Berger (87) critically reviews current knowledge of the effects of scattering on penetration and applies it to an analysis of experimental curves (78, 143) of detector response versus thickness of particle absorber. The analysis accounts for the major part of the curves though not for their behavior in the direction of short penetration.

7. Phenomena Associated with Particle Tracks

The study of particle penetration in a material is traditionally associated with numerous effects, such as ionization or luminescence, which serve to detect the particle's passage and to provide information on its charge, mass, energy, etc. As the study of these processes progresses, it often bears increasingly on atomic properties of the material and less on the primary interaction of the particle. Thus this study develops into a number of separate chapters of physics, each of them of interest in its own right and with far-reaching ramifications, even while it remains relevant to particle penetration. In this section a number of associated effects will be mentioned, to give some indication of their present development and some reference to more detailed reports.

The effects of a particle that come under observation are, in general, rather remote from the initial particle collisions. The collection of ions affords plenty of time for their chemical transformation (e.g. $H_2^+ + H_2 \rightarrow H_3^+ + H$). Numerous processes—known and unknown—convert excitations into ionization. Light emission almost never proceeds from the levels of initial excitation. The often strikingly simple quantitative relationships between the energy lost by a particle and its observable effects, which emerge from experimental studies with moderate accuracy, may suggest, deceptively, a close link between these effects and the initial collisions, whereas the actual complexity of intervening events emerges only from more sophisticated tests.

7.1 *Energy deposition along particle tracks.*—Some of the energy lost by a fast charged particle is removed from the vicinity of its track within times $\lesssim 10^{-15}$ sec by fast secondary electrons or by Cerenkov radiation. To analyze the operation of detectors, one often wants to distinguish the energy left near the track ("restricted energy loss") from the total energy loss. The definition of restricted energy loss depends on the circumstances of interest. If often excludes the energy spent in producing secondary electrons with

initial energy in excess of a suitable limit T_0 and the Cerenkov radiation with frequency below that of the lowest absorption band of the material (higher frequency Cerenkov radiation is absorbed rapidly [Sternheimer (119), Budini & Taffara (34)]). Assuming that $Q=T_0$ lies in the range of the high-Q approximation, the theory excludes fast secondaries by replacing the integration limit $Q_{\max}$ with T_0 in Equation 37. To exclude the energy removed by Cerenkov radiation, one calculates separately the integral of the second term on the right-hand side of Equation 47 over the frequency band where ϵ_2 is negligible and the arctangent is near π. One finds then, instead of Equation 38,

$$\left(-\frac{dE}{ds}\right)_{\text{restr.}} = \frac{2\pi z^2 e^4}{mv^2} NZ \left\{ \ln \frac{2mv^2 T_0}{I^2} - \frac{1-\beta^2}{2mc^2} T_0 + \ln \frac{1}{1-\beta^2} - \beta^2 - 2\frac{C}{Z} - \delta - \Delta_C \right\} \quad 88.$$

where

$$\Delta_C = \frac{1}{\omega_p^2} \int_{Im\,\epsilon=0,\,\epsilon\beta^2>1} 2\omega d\omega \left[\beta^2 - \frac{1}{\epsilon(\omega)}\right] \quad 89.$$

remains below 1 in H_2 and He, below 0.1 in other gases and, ~ 0.01 in solids [Sternheimer (140, pp. 8–10)].

The restricted energy loss has a finite limit at high energy, called the "Fermi plateau," which is, owing to Equation 50,

$$\left(-\frac{dE}{ds}\right)_{\text{restr.. }\beta=1} = \frac{2\pi z^2 e^4}{mv^2} NZ \left\{ \ln \frac{2mc^2 T_0}{(\hbar\omega_p)^2} - \left(2\frac{C}{Z} + \Delta_C\right)_{\beta=1} \right\}$$

$$= 0.154 \frac{Z}{A} \left\{ \ln \frac{1400 (T_0)_{\text{eV}}}{(\rho)_{\text{g cm}^{-3}} Z/A} - \left(2\frac{C}{Z} + \Delta_C\right)_{\beta=1} \right\} \text{MeV g}^{-1}\,\text{cm}^2 \quad 88a.$$

where $(2C/Z+\Delta_C)_{\beta=1} \ll 1$ in all materials but H and He.

Extensive experimental verification of this formula has been obtained [see, e.g., Sternheimer (140, pp. 20–40)]. However, doubts have been cast on it recently by experiments at $E>100\ Mc^2$ with nuclear emulsions [Alekseyeva et al. (2), Zhdanov et al. (141)] which show a decrease of $(-dE/ds)_{\text{restr.}}$ by 5–10 percent in this extreme relativistic range. Tsytovich's theoretical work [(129); see Sec. 2.13] accounts for this result in terms of radiative corrections. This matter remains unsettled at the moment as an attempt to reproduce the experiment has pointed to possible disturbing influences in the handling of the emulsions [Stiller (125)].†

† *Note added in proof.* Continued experimentation by Stiller and Herz (private communication) with various types of nuclear emulsion exposed and treated under strictly controlled conditions has failed to demonstrate a systematic uniform trend of the blob density count at $E>100\ Mc^2$. On the contrary, this work has emphasized differences in the behavior of different emulsions and thereby suggests that the blob density may not correlate with $(-dE/ds)_{\text{restr.}}$ to provide an adequate test of the theory.

7.2 *Delta rays.*—Delta rays are secondary electrons of energy sufficient to cause their track to fork out detectably from the heavy-particle track or to be otherwise noticeable. The minimum energy T_0 required for this classification depends of course on experimental criteria. If the high-Q approximation holds for $Q > T_0$, the number of δ rays of energy T produced per cm of track is given by a formula analogous to Equation 31

$$d\mathfrak{N}_T = \frac{2\pi z^2 e^4}{mv^2} NZ \left(\frac{1}{T^2} - \frac{1 - \beta^2}{2mc^2 T} \right) dT \qquad 90.$$

This formula serves well to determine the z and v of a particle on the basis of its δ-ray production because all its elements are well defined. However, an excess of δ rays over the prediction of Equation 90 occurs at energies T that are not much larger than the binding energy of atomic electrons, because the high-Q approximation no longer holds. This increase, which is responsible for the second term of Equation 72, has not been studied quantitatively.

7.3 *Primary ionizations and excitations.*—Successive ionizing collisions occur far enough apart along the track of a fast particle for the particle to frequently traverse a low-pressure counter without causing any ionization and, therefore, any discharge. This circumstance offers an opportunity to measure the frequency of primary ionizations along a track [McClure (74)]. The great majority of collisions involve a small momentum transfer, even though high-Q collisions contribute about half of the total energy loss. Accordingly, measurements of the number $\mathfrak{N}_I$ of ionizing collisions per centimeter of track provide information on the parameters of the low-Q approximation, i.e., on the dipole strengths $|(\Sigma_j x_j)_{n0}|^2$ of Equations 22 and 23. The plot of $\beta^2 \mathfrak{N}_I$ versus the velocity function $\ln[\beta^2/(1-\beta^2)] - \beta^2$, which appears in Equation 35, is a straight line (within the limits of the Born approximation) whose slope measures the quantity

$$M_i^2 = \Sigma_{n \text{ ionized}} |(\Sigma_j x_j)_{n0}|^2 \qquad 91.$$

[Fano (41)].

Platzman (97) has emphasized that the set of ionized states over which the sum is performed in Equation 91 does not coincide with the set of all states whose energy E_n exceeds the ionization threshold E_i of the molecule in the collision. Final states of molecules with $E_n > E_i$ may be dissociated, for example, rather than ionized. On the other hand, excitation to states with $E_n < E_i$ may result in eventual ionization of another molecule with a lower E_i. In order to avoid classifying the states n according to their eventual properties, Platzman writes Equation 91 in the form

$$M_i^2 = \Sigma_n |(\Sigma_j x_j)_{n0}|^2 \eta_n \qquad 91a.$$

where η_n is the probability that the state n leads to ionization.

This method of analysis of collision cross sections has been applied to correlate the optical transition parameters $|(\Sigma_j x_j)_{n0}|^2$ and the cross sections

for excitation to specific levels n by electron collisions (82, 101). Figure 7 gives an example of this plot and provides, incidentally, a verification of the Born approximation collision theory over a large range of energies. The drop of the experimental points below the straight line at low energies represents the failing of the Born approximation. The shape of the curve in Fig. 7 is, of course, characteristic for optically allowed transitions from the ground

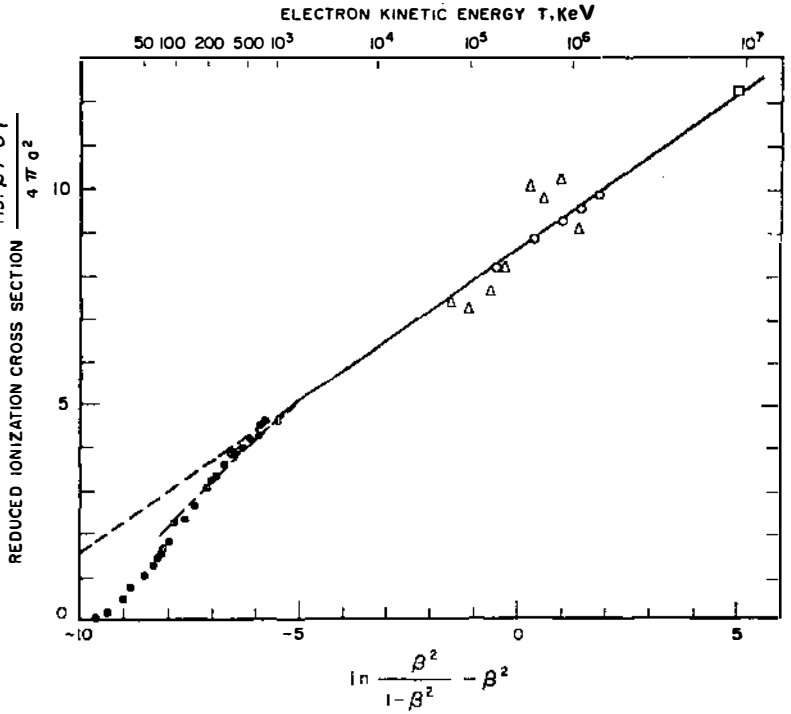

FIG. 7. Ionization of H_2 by electron bombardment. Experimental data: △ Williams & Terroux (1930), ● Tate & Smith (1932), □ Danforth & Ramsey (1936), ○ McClure (1953)

– – – —— Theoretical asymptotic law

$$(137\beta)^2\sigma_i/\pi a^2 = 0.711\ \{\ln[\beta^2/(1-\beta^2)] - \beta^2\} + 8.63$$

—·—·— The same, corrected for exchange (100)

The coefficient 0.711, determined by fitting the theoretical law to experimental data, measures M_i^2 in units of the squared Bohr radius a^2. (Courtesy R. L. Platzman.)

state to the state n. The cross sections for forbidden transitions with $\Delta L \neq 1$ vanish in the low-Q approximation and therefore fail to rise linearly on the right of the figure but flatten out at a constant level.

7.4 *Ionization yield.*—The ionization chambers, which are the classic particle detectors, the proportional counters, which are ionization chambers with internal amplification, and the semiconductor counters respond to the passage of a heavy particle in proportion to the number of charge pairs separated in their sensitive volume. This number of charges is closely proportional to the energy dissipated, and the proportionality constant depends but little on the characteristics of the particle. The constant is usually expressed as the energy W dissipated per pair of ions produced. The quantity W is understood to represent a grand average over a large number of ionization processes produced by the incident particle, by secondary electrons, and by subsequent intermolecular processes.

Much effort has been devoted over the years to the study of W in gases. [See, e.g., the reviews by Boag (20), Valentine & Curran (131), Booz & Ebert (26), and Whyte (138).] The data shown in Table III pertain mostly to α particles and β rays. The values for 340-MeV protons are a little lower than those for α particles, but this difference is probably not significant. The data for electrons show values of W a few percent lower than those for α particles except in hydrogen and in the noble gases; achievement of accurate, absolute measurement of W for β rays (60) has represented considerable progress. The excess of W over the energy I_0 actually required to produce an ionization represents, of course, a diversion of energy to excitation and to other processes. For the monoatomic rare gases W/I_0 lies near 1.7 to 1.8; for the molecular gases, in which excitation is comparatively more likely and in which energy may go into molecular potential to yield dissociation or vibrational excitation, this ratio ranges from 2.1 to 2.6.

The remarkable stability of W against changes of velocity of the incident particles derives in part from the small influence of the velocity on the relative cross section for different types of excitation or ionization collisions. It is enhanced by the circumstance that excess energy imparted to fast secondary electrons can be utilized for the production of further ionization by these electrons; moreover, the energy distribution of these secondaries also depends weakly on the velocity of the incident particle. Other compensating factors which remain unidentified presumably operate. Platzman (87, 98) has achieved considerable progress in analyzing the distribution of the incident energy between ionization and other processes throughout the sequence of secondary phenomena. In the case of He, a theoretical calculation of the whole chain of events has been successfully completed (82, 98)[40] yielding $W=43$ eV, in very good agreement with experiments.

The study of W in gases has taken a new turn since the discovery of the

[40] This calculation requires a good knowledge of the collision cross sections for slow secondary electrons. The assembly of these data for helium (82) raised a major obstacle which has not yet been overcome for other gases except H_2. An earlier calculation by Erskine (39) utilized unrealistic cross sections.

TABLE III

VALUES OF W (eV/ion pair)

	Substance	α Rays	340-MeV protons	β Rays
Gases				
	He	42.7 (59) 46.0 (27)		42.3 (60)
	Ne	36.8 (59)		36.6 (60)
	Ar	26.4 (59, 27) 26.25 (53)		26.4 (60)
	Kr	24.1 (59)		24.2 (60)
	Xe	21.9 (59)		22.0 (60)
	H_2	36.3 (59) 37.0 (27) 36.0 (12)	36.5 (3)[a]	36.3 (60)
	N_2	36.38 ± 0.07 (8) 36.39 ± 0.07 (62) 36.50 (12)	34.7 (3)[a]	34.9 (61)
	O_2	32.5 (59) 32.2 (53) 32.2 (27)	32.6 (3)[a]	30.9 (60)
	Air	34.97 ± 0.07 (8) 34.96 ± 0.07 (62) 34.95 (12)	34.4 (3)[a]	33.8 ± 0.2 (26) (>20-keV average)
	CO_2	34.04 (8) 34.3 (27) 34.3 (12)		32.9 (60)
	CH_4	29.0 (12) 29.2 (59) 29.4 (27)		27.3 (61)
Solids				
	Si	3.55 (86)		3.55 (65)
	Ge	2.9 (86, 79, 75)		
	Se	3.9 (79)		
	InSb	0.6 (127)		
	AgCl			7.6 (132)

Note—Experimental error estimates are indicated only where they are particularly low or otherwise significant.

[a] These values were adjusted to make $W_{Ar}=26.4$ eV.

Jesse effect, namely, of the extreme sensitivity of W in He to trace impurities which ionize upon collision with excited He atoms. The same effect occurs in Ne and, to a lesser extent, in Ar. The ionization yield has now become an indicator of the comparative probability of ionization and other molecular processes and of the energy exchanges among molecules in a gas. Following Platzman's observation that ionization in molecules is subject to competition with dissociation (97) and that the speed of dissociation is affected adversely by replacement of atoms with their heavier isotopes, Jesse has demonstrated that replacement of hydrogen with deuterium reduces the value of W [Jesse & Platzman (63)].

In semiconductor counters only $\sim$1 eV is required to lift an electron to the conduction band, as compared with the 10–20 eV required to ionize a gas molecule. Accordingly the ionization yield in semiconductors is much higher than in gases, and corresponds to a value of $W \sim 3$ eV. This value has been accounted for remarkably well by a simple model of the mechanism through which the energy lost by a fast particle is converted to produce ionization in a solid [Chynoweth, Schweinler (86), Shockley (110)]. This model considers only the excitation of individual electrons to the conduction band by the passage of a fast particle and the subsequent chainwise excitation of other electrons if the one first excited had received sufficient energy. On the other hand, the evidence presented in Section 2.10 indicates that the main excitations in metals and semiconductors are of the collective ("plasma") type and have energy levels much higher than 1 eV. Thus the mechanism that controls the value of W in solid counters may require further clarification.

7.5 *Grain and bubble counts; luminescence.*—Other modern particle detectors, namely, photographic emulsions, bubble chambers, and scintillators, give a response that is closely related to the particle's energy loss but depends also appreciably on its velocity. The number of grains that appear along a particle track in an emulsion (after it has been developed), the number of bubbles in a bubble chamber, and the amount of light that emerges from a scintillator per centimeter of track depend, like gas ionization, on sequences of secondary processes. However, the circumstances for maintaining a stable response per unit energy loss are not quite as favorable here as for gas ionization.

Much effort has been devoted to studying the energy loss of heavy particles at relativistic velocities indirectly through grain or bubble counts and through the light output of scintillators. This effort was reviewed in considerable detail a few years ago (140, see particularly pp. 21–38 by Sternheimer). As an indication of order of magnitude, one "blob" (i.e., grain or group of grains) is observed per 10^3 eV of energy dissipation, one bubble per $3\text{–}5 \times 10^3$ eV in most of the relevant materials, and one scintillation photon per 10^2 eV.

Each grain or bubble may stem, at least for high-speed particles, from a single collision. Collisions involving different amounts of energy loss are not

equally effective in producing grains or bubbles. This fact alone would not spoil the proportionality of grain or bubble count to the energy loss if the relative frequency of different types of collision were independent of the particle's velocity. As can be seen from the theory of energy losses developed in Section 2, the relative frequency of collisions produced by the longitudinal interaction remains remarkably constant as the particle velocity varies, because it varies at most as the logarithm of the velocity. However, the rising contribution of the transverse interaction at relativistic energies introduces an appreciable change in the spectrum of energy losses because this interaction yields no intermediate-Q collisions (Sec. 2.4) and therefore very few δ rays of low or moderate energy.

This difference between the collisions produced by transverse and longitudinal interactions has a characteristic effect [Barkas (5)]. The production of a bubble appears to require a fair amount of energy, of the order of 300–1000 eV, and thus to depend particularly on the occurrence of low energy δ rays.[41] In hydrogen, which contains no inner-shell electrons, δ rays of this energy cannot arise from low-Q collisions. The frequency of these δ rays along the track is then given approximately by the first term of Equation 90 (since $T \ll mc^2$) and amounts to $25/\beta^2$ per centimeter for the total production of δ rays with $T > 400$ eV. Careful experimental studies [see e.g. Kenney (64), Sechi-Zorn (142)] have confirmed the β^{-2} law, and thus the absence of any relativistic rise of the bubble count in H_2, within the theoretical and experimental accuracy. (This bubble count amounts to $8.5/\beta^2$ cm^{-1}.) Other liquids, however, contain inner-shell electrons which can be ejected in low-Q collisions with $E_n > 300$ eV. Therefore, the frequency of these collisions should show a relativistic rise, arising from the contribution of the $\ln[1/(1-\beta^2)]$ term in Equation 32. A relativistic rise of 5 percent has actually been observed in propane [Blinov et al. (16)] and a much larger one of 30 percent has been reported for the heavier liquid $CBrF_3$ [Hahn & Hughentobler (54)].

Similar effects might also influence emulsion grain counts, but to a smaller extent because of the presumably lower threshold for grain development than for bubble formation. At any rate, the blob density along high energy particle tracks has been found to parallel closely the restricted energy loss (Eq. 88), with T_0 of the order of a few keV. The blob density exhibits a relativistic rise of the order of 15 percent from the minimum, at $E \sim 4\ Mc^2$, to the "plateau" at $E > 100\ Mc^2$ [see e.g. (140, p. 15), Shapiro (109), Patrick & Barkas (93)]. Notice, however, that the calculated magnitude of this rise is

[41] Dr. A. G. Tenner kindly points out that the amount of energy actually spent in bubble formation is only ~10 eV in hydrogen and helium, even though the transfer of a much larger amount of energy to a δ ray is probably necessary. He also points out that the interpretation given here of the absence of relativistic rise for the bubble count in liquid hydrogen implies the still unverified assumption that a rise should be observed for the restricted energy loss. Dr. Tenner has carried out a detailed study of the mechanism of bubble formation (145).

rather sensitive to the assumed values of I and T_0, because it is small as compared to the separate values of the minimum and the plateau. (See also the remarks on recent experiments at the end of Sec. 7.1.)

In the process of scintillation, the output of light is influenced greatly by the competing phenomena of dissociation, intermolecular energy exchanges, and radiationless de-excitation, wherein electrons return to lower states, transferring excess energy to molecular vibrations. The competition among alternative processes depends on the concentration of energy deposited along a particle track, particularly in organic scintillators. Light emission is least efficient along the tracks of slower particles where the energy concentration is highest. For example, along a proton track in anthracene the light output per kilo electron volt of energy dissipation decreases from 15 to 5 photons as the proton's energy drops from 100 to 1 MeV (140, p. 127). A disproportionately large fraction of the light emitted along heavy-particle tracks may be contributed by δ-ray branch tracks [Galanin (50), Murray & Meyer (84)].

In many scintillator materials the light is emitted by activator impurities (e.g., by Tl atoms in NaI crystals, by terphenyl in polystyrene), excited by transfer from molecules of the bulk material which have a somewhat higher excitation level. Whether these excitations of the bulk material ($\sim$5 eV in organic scintillators) are closely or remotely related to the collisions of charged particles is still unknown, even though substantial effort has been devoted to study of this question. It is of the essence, in this connection, that the majority of collisions lead to rather high (10–20 eV) excitations, whose study is barely getting under way [see e.g. Platzman (99)].

7.6 *Boundary effects.*—When a fast charged particle traverses the surface of a material (or, more generally, the boundary between any two media), it may experience energy losses that are not otherwise observed during its penetration of the homogeneous portions of the same material. These energy losses are small, of the order of 5 eV, and therefore contribute insignificantly to the overall slowing down of the particle. The formation of a thin oxide film on the surface has, of course, a substantial effect on the magnitude of such an energy loss and on the subsequent phenomena that derive from it.

Macroscopically, as a particle approaches a surface, it induces on it a charge distribution of opposite sign; the combination of the incident and induced charges constitutes a variable dipole which emits a "transition radiation" [Ginzburg & Frank (51)]. Microscopically, the separation of longitudinal and transverse excitations (Sec. 2 3), which hinges on the isotropy of a material, breaks down in the presence of a boundary. Levels of electronic excitation occur which are neither longitudinal nor transverse but are localized near boundaries and have a spectrum different from that of the collective excitations in bulk material discussed in Section 2.10 [Ritchie (103), Ferrell et al. (46); for experimental evidence see Powell (102)]. Thus one speaks of "surface plasmons" in opposition to "volume plasmons," both of them being low-q excitations of the outer atomic electrons influenced pro-

foundly by electrostatic interaction of electrons over distances of the order of 10^{-6} cm. The surface plasmons may decay through the emission of optical radiation from the surface [Ferrell (47)]. This emission has been discovered [Steinmann (116), Brown et al. (33)] and shown to coincide, at least in essence, with the macroscopic transition radiation [Silin & Fetisov (111), Stern (117)].

The surface effects are, of course, particularly accessible to observation when the volume effects are minimized by reducing the total thickness of material. In fact, they have generally been studied through experiments with thin films. However, the occurrence of two film boundaries at a short distance complicates the situation, and detailed understanding of the observations requires thorough experimental and theoretical analysis [Boersch et al. (21), Frank, Arakawa & Birkoff (48), Ritchie & Eldridge (104)].

8. Summary of Tabulations and Formulas

Interpretation of recent information on the stopping power and ranges of mesons, protons, deuterons, and α particles is based mostly on Equations 38 and 39, or on the related Equation 86 for the restricted energy loss, complemented by experimental data. Tabulations differ in general in the values assumed for I, C, and δ. Of these quantities, I has been discussed in Section 3 and C in Section 4; the practical evaluation of δ is described in Section 8.1. Suggested values of I and C/Z are given in Table I and Figure 6, respectively.

Because of the considerable uncertainties on the values of I and C in recent years, the trend is to allow the user maximum flexibility in the choice of these values. To this end, the user may be supplied either with only the raw Equation 38, or with tabulations of parts of this formula, or with more complete tabulations for specified values of I, rather than for specified materials. Evaluation of the formulas is discussed in Section 8.2, the main recent tables in Section 8.3.

The reader is reminded here that the stopping power at lower velocities, at which capture and loss of atomic electrons is frequent, has not been treated in this article. Some information on this subject is given in Section 8.4, and on the related stopping power of fast heavy ions in the companion article by Northcliffe (91).

Semiempirical range-energy formulas, usually of the type $R=aE^b$, have been frequently employed. Their connection with the theoretical formulas will be indicated in Section 8.5.

8.1 *Calculation of* δ.—The density effect correction δ is defined by Equation 48 as an integral in terms of the dielectric constant at all frequencies. The method of evaluation of this integral has been indicated in note 17. Sternheimer (118) has found it adequate and convenient to represent δ by the approximate analytical expressions

$$\delta = 0 \qquad \text{for } X < X_0$$
$$\delta = 4.606X + C + a(X_1 - X)^m \qquad \text{for } X_0 \leq X \leq X_1$$
$$\delta = 4.606X + C \qquad \text{for } X > X_1$$
$$X = \log_{10}(p/Mc) = \tfrac{1}{2}\log_{10}[\beta^2/(1-\beta^2)] \qquad 92.$$

where the parameters a, m, C, X_0, and X_1 have to be given for each material and depend on its dielectric constant.[42] This procedure has been in general use, with somewhat different values of the parameters, depending on the assumed value of I. Notice that the term 4.606 X merely cancels $\ln[\beta^2/(1-\beta^2)]$ in Equation 38 and that $-C = 2\ln(I/\hbar\omega_p) + 1$, owing to Equation 50. Current values of the parameters are given in Table IV.

8.2 *Evaluation of the stopping power formula.*—Bichsel (14) has cast expression 38 into the form

$$-\frac{dE}{ds} = z^2\frac{Z}{A}K(\beta)\left\{f(\beta) - \ln(I)_{\text{eV}} - \frac{C}{Z} - \tfrac{1}{2}\delta\right\}\text{MeV g}^{-1}\text{cm}^2$$
$$K(\beta) = 0.307/\beta^2$$
$$f(\beta) = \ln[1.022 \times 10^6\beta^2/(1-\beta^2)] - \beta^2 \qquad 93.$$

and has given a table of K, f, and β as functions of a proton's kinetic energy. As elsewhere in this article, z is the incident particle's charge in units of e;

TABLE IV

PARAMETERS FOR STERNHEIMER'S EQUATION 92

(Courtesy S. Seltzer)

Z	I(eV)	$-C$	a	m	X_1	X_0
4	64	2.83	0.413	2.82	2.0	−0.10
13	164	4.21	0.0906	3.51	3.0	0.05
29	315	4.38	0.107	3.39	3.0	0.17
47	475	5.09	0.183	3.05	3.0	0.02
82	805	6.16	0.344	2.66	3.0	0.39
92	894	5.89	0.318	2.66	3.0	0.20

$v = \beta c$ represents its velocity; Z/A is the number of electrons per atomic weight unit of the material; I can be taken or interpolated from Table I; C/Z can be read or interpolated from Figure 6; and δ can be calculated from Equation 92 and Table IV. Equation 88 becomes, in a form analogous to Equation 93,

$$\left(-\frac{dE}{ds}\right)_{\text{restr.}} = z^2\frac{Z}{A}K(\beta)\left\{\frac{1}{2}f(\beta) - \ln(I)_{\text{eV}} + \frac{1}{2}\ln(T_0)_{\text{eV}} - 0.489 \times 10^{-6}(1-\beta^2)(T_0)_{\text{eV}} - \frac{C}{Z} - \frac{1}{2}\delta - \frac{1}{2}\Delta_C\right\}\text{MeV g}^{-1}\text{cm}^2 \qquad 94.$$

[42] The parameter C in this paragraph is, of course, unrelated to the shell correction indicated by the same symbol.

Approximate analytical formulas to represent C have been given recently by Bichsel (14) and Barkas (7). In Bichsel's work (see Sec. 4.3) an analytical formula with adjusted parameters represents the contribution of each atomic shell or subshell to C. Barkas utilizes an empirical polynomial expression in two variables, $C = F(\eta^{-2}, I)$, which depends on the particle energy through $\eta^2 = \beta^2/(1-\beta^2)$ and on the properties of the material through the mean excitation energy I. (This expression has been designed to yield an adequate fit for the total range, but not necessarily for the stopping power; it has been used for $\eta > 0.13$ only.) Both the Bichsel and Barkas expressions of C are adjusted to vanish in the high energy limit, whereas C actually remains finite in this limit (see Sec. 4.4). However, this discrepancy is hardly significant at the current level of accuracy, because $(C/Z)_{v=c} < 0.05$ whereas $f(1) + \cdots$ in Equation 93 exceeds 5.

8.3 *Tables of stopping power and range.*—The most recent tables in regular publication channels appear to be those of Sternheimer (89, 122, 140). These tables provide a good coverage of the subject but two ingredients of their preparation have proved to be inaccurate,[43] namely, the "high" I values ($I/Z \sim 13$ eV), akin to those of (36), and the assumption $C \sim C_K + C_L$, i.e., C_M, etc. ~ 0. Adaptation to improved I values was made possible in (124) by the development of interpolation procedures. These tables extend to a proton energy of 100 GeV.

Still in the "report" stage are two more recent tabulations by Bichsel (14) and Barkas (7), which rest on essentially the same input data and, therefore, differ only in format and in minor details. Bichsel's tables pertain to a set of specific materials and include both stopping power and ranges for proton energies up to 700 MeV.[44] Barkas' single main table gives ranges for proton energies up to 5 GeV. The density effect is not taken into account in this table, but can be corrected for by means of a subsidiary table. Barkas represents the proton range as a smooth universal function of two variables, the proton energy (or velocity) and the mean excitation energy I of the material, and has designed his table for interpolation in both variables. To achieve smoothness, Barkas' main table gives the range in "moles of electrons per cm^2," conversion to g/cm^2 being achieved by multiplication by A/Z (chemical atomic weight per electron). Another extensive table of ranges and stopping power has been prepared recently in report form by Williamson & Boujot (144); this table assumes $I = 13.02\ Z$ eV for $Z > 5$ and takes into account only the K-shell contribution to shell corrections.

All these range tables can be applied to mesons, hyperons, deuterons, and α particles in accordance with Equation 40; Barkas (7) gives a table of the scale parameter M/z^2. The effect upon the range of electron capture and loss

[43] Improved data on Cu and Pb have been calculated by Dr. Sternheimer [private communication and (122) "Errata"].

[44] Bichsel calls "pathlength" the quantity called "range" in this article and "range" the "projected range" (depth of penetration).

in the terminal section of the path is represented by Barkas as follows. He characterizes the main range data as pertaining to idealized particles with $M/z^2=1$ which do not capture electrons, and then represents the departure from the "idealized" particle range observed for protons or other heavy particles by an additional corrective term $(M/z^2)B_z$. The determination of B_z is an important goal of the studies of electron capture and loss (see Sec. 8.4).

Brandt's report (30) contains a very extensive table of stopping powers and ranges, with particular emphasis on organic compounds. The values of I underlying these tables are much lower than the currently accepted values for $Z>25$; for organic compounds the I values were obtained by theoretical procedures referred to in Section 3.2.

8.4 *Low energy effects of electron capture and loss.*—Empirical range-energy relations, usually in the form of power laws, have been used in the past at low energies where the stopping power theory described in this article breaks down. Recently the trend has emerged to provide the user with extensive range and stopping power tables derived by interpolation from experimental data. Extensive tables of this type for protons from .04 to 10 MeV and for α particles from 3 to 40 MeV have been prepared by Whaling (137).[45] A smaller table of proton ranges, based primarily on new measurements, has been given by Rybakov (106).[46]

For α particles, electron capture is already appreciable at several MeV and is very important at 800 keV. (However, rough data presented by Whaling (137) indicate no significant, ± 20 per cent, influence on stopping power above 1.6 MeV.) Spot comparison of Whaling's α-particle and proton ranges indicates departures from the scaling law 40 of the order of 10 per cent for α particles of energy as high as 8 MeV. The α-particle ranges show here an extension, due to reduced stopping power at lower energies when their charge is reduced by electron capture. Data by Heckman et al. (4) on the corresponding extension for heavier ions indicate, in agreement with Whaling's tables, that the range extension for α particles, B_2, has reached its maximum value at 4 MeV, i.e., that the stopping power theory should apply above this energy. [In emulsion B_z is found (4) to be $\sim z^{8/3}g(137\beta/z)$ where g increases almost linearly from $\beta=0$ to $\beta\sim 20z/137$ and thereafter remains constant at $\sim .2$ μ.] This problem is highly relevant to the accompanying article by Northcliffe (91).

8.5 *Semiempirical range formulas.*—Substitution of the stopping power expression 93 into the range formula 39 yields

[45] Caution is indicated in the use of these tables for protons in the 1–10 MeV range, because they are based largely on experimental data at lower energies and on extrapolation by means of a semitheoretical formula with no shell corrections.

[46] Rybakov's "ranges" represent depth of penetration; a correction (Sec. 6) is required to obtain pathlengths from them.

$$(R)_{\text{g cm}^{-2}} = 3.25 \frac{A}{z^2 Z} \int_0^{E_0} \frac{\beta^2}{\{f(\beta) + \cdots\}} d(E)_{\text{MeV}} \qquad 95.$$

By replacing the slowly varying function $f(\beta) + \cdots$ with a suitable average value, as a first approximation, one obtains

$$(R)_{\text{g cm}^{-2}} \sim 3.25 \frac{A}{z^2 Z} \frac{1}{\langle f(\beta) + \cdots \rangle} \left(\frac{E_0^2}{E_0 + Mc^2} \right)_{\text{MeV}} \qquad 95a.$$

namely, a quadratic dependence of R on the initial kinetic energy E_0 in the nonrelativistic range of energies and a linear dependence in the extreme relativistic range. The transition between these two laws of variation is gradual. This transition is made still smoother when one evaluates Equation 95 taking into account the variation of $f(\beta) + \cdots$, by the circumstance that $f(\beta) + \cdots$ actually increases faster at lower energies, where β^2 also increases, and more slowly at higher energies.

These considerations make it plausible that a plot of $\ln R$ versus $\ln E_0$ exhibits only a small curvature and that appreciable portions of it can be approximated rather accurately by straight lines

$$\ln R = \ln a + b \ln E_0 \qquad \text{(i.e., } R = aE_0^b\text{)} \qquad 96.$$

The slope b lies between 1 and 2 and decreases slowly as E_0 and R increase.

The value $b = 1.75$ has, for example, been utilized for an application to protons up to 300 MeV (78) (see p. 47). Recently Seb (108) has fitted proton ranges in photographic emulsions satisfactorily by means of Equation 96, taking $b = 1.74$ between 7 and 200 MeV and 1.52 between 200 and 1000 MeV. Seb also presents evidence that range-energy curves for different materials are fitted by Equation 96 with the same value of b and with a varying in proportion to I^{-b}. Thereby the range in all materials would be represented by a universal function of the ratio E_0/I. Inspection of the curves in Figure 5 shows that, first, the curves for different materials lie close to one another and, second, they would be pushed still closer over a broad range if the scale of abscissas were changed from $x = v^2/v_0^2 Z$ to $x' = 2mv^2/I$. This last scale would cause the curves to coincide for large x'. On the other hand, inspection of Figure 6, which provides an enlarged view of the differences among materials, shows that no really universal range-energy relation exists. Equation 95a emphasizes that the energy ratio E_0/Mc^2 is highly relevant, Seb emphasizes the relevance of E_0/I and Section 4.4 the relevance of the velocity ratio of the incident particle and atomic electrons, which differs somewhat from E_0/I. In view of these circumstances, a judicious exploitation of the gross simplifying features, of theoretical knowledge, and of empirical fitting of parameters to critical experimental data might well yield, in the next few years, stopping power and range formulas that meet all reasonable tests of simplicity, accuracy, and adherence to relevant physical circumstances.

LITERATURE CITED

1. Agranovich, V. M., *Fiz. Tverd. Tela*, **3**, 811 (1961) [Transl., *Soviet Phys.-Solid State*, **3**, 592 (1961)]
2. Alekseyeva, K. I., Zhdanov, G. B., Zamchalova, E. A., Novak, M., Tretyakova, M. I., and Shcherbakova, M. N., *Proc. III Intern. Conf. Nucl. Photography, Moscow, 1962*, 396; Alekseyeva, K. I., Zhdanov, G. B., Tretyakova, M. I., Tsytovich, V. N., and Shcherbakova, M. N. *IV, Intern. Koll. Korpuskularphot., München, 1963* (In press)
3. Bakker, C. J., and Segrè, E., *Phys. Rev.*, **81**, 489 (1951)
4. Barkas, W. H., *Nuovo Cimento*, **8**, 201 (1958); also Heckman, H. H., Perkins, B. L., Simon, W. G., Smith, F. M., and Barkas, W. H., *Phys. Rev.*, **117**, 544 (1960)
5. Barkas, W. H., *The Velocity Dependence of Bubble-Track Density, Univ. Calif. Radiation Lab. Rept. 9420* (1960)
6. Barkas, W. H., and von Friesen, S., *Nuovo Cimento, Suppl.*, **19**, 41 (1961)
7. Barkas, W. H., *The Range-Energy Function, Univ. Calif. Radiation Lab. Rept. 10292* (1962); to be superseded by ref. (87)
8. Bay, Z., Newman, P. E., and Seliger, H. H., *Radiation Res.*, **14**, 551 (1961)
9. Berger, M. J., *Methods in Computational Physics*, 1 (Alder, B., Fernback, S., and Rothenberg, M., Eds., Academic, New York, 1963)
10. Bethe, H. A., *Ann. Physik*, **5**, 325 (1930); *Handb. Physik*, **24/1**, 491 ff. (Springer, Berlin, 1933)
11. Bethe, H. A., *Phys. Rev.* **89**, 1256 (1953)
12. Biber, C., Huber P., and Müller, A., *Helv. Phys. Acta*, **28**, 503 (1955)
13. Bichsel, H., and Uehling, E. A., *Phys. Rev.*, **119**, 1670 (1960)
14. Bichsel, H., *Passage of Charged Particles through Matter, Univ. So. Calif. Rept. No. 2* (Contract AT(04-3)-136, 1961) (In press as Sec. 8c of *Handbook of Physics*, 2nd ed., McGraw-Hill, New York, 1963); *Higher Shell Corrections in Stopping Power, Univ. So. Calif. Rept. No. 3* (Contract AT(04-3)-136) (1961)
15. Blanchard, C. H., *Natl. Bur. Std. (U.S.), Circ. 527*, 9 (1954)
16. Blinov, G. A., Krestnikov, Iu. S., and Lomanov, M. F., *Soviet Phys. JETP (Engl. Transl.)*, **4**, 661 (1957)
17. Bloch, F., *Z. Physik*, **81**, 363 (1933)
18. Bloch, F., *Ann. Phys. (Leipzig)*, **16**, 285 (1933)
19. Blunck, O., and Leisegang, S., *Z. Physik*, **128**, 500 (1950)
20. Boag, J. W., *Quantities, Units and Measuring Methods of Ionizing Radiation* (Fossati, F., Ed., Hoepli, Milano, 1959)
21. Boersch, H., Radeloff, C. and Sauerbrey, G., *Phys. Rev. Letters*, **7**, 52 (1961)
22. Bohm, D., and Pines, D., *Phys. Rev.*, **92**, 609 (1953)
23. Bohr, A., *Kgl. Danske Videnskab. Selskab, Mat.-Fys. Medd.*, **24**, (19) (1948)
24. Bohr, N., *Phil. Mag.*, **30**, 581 (1915)
25. Bohr, N., *Phil. Mag.*, **25**, 10 (1913); *Kgl. Danske Videnskab. Selskab, Mat.-Fys. Medd.*, **18**, (8) (1948)
26. Booz, J., and Ebert, H. G., *Strahlentherapie*, **120**, 7 (1963)
27. Bortner, T. E., and Hurst, G. S., *Phys. Rev.*, **93**, 1236 (1954)
28. Brandt, W., *Phys. Rev.*, **104**, 691 (1956)
29. Brandt, W., *Phys. Rev.*, **111**, 1042 and **112**, 1624 (1958)
30. Brandt, W., *Phys. Rev.*, **112**, 1624 (1958); *Energy Loss and Range of Charged Particles in Matter* (du Pont Co. Rept., 1960)
31. Brolley, J. R., and Ribe, F. L., *Phys. Rev.*, **98**, 1112 (1955)
32. Brown, L. M., *Phys. Rev.*, **79**, 297 (1950)
33. Brown, R. W., Wessel P., and Trounson, E. P., *Phys. Rev. Letters*, **5**, 472 (1960)
34. Budini, P., and Taffara, L., *Nuovo Cimento*, **4**, 23 (1956)
35. Burkig, V. C., and MacKenzie, K. R., *Phys. Rev.*, **106**, 848 (1957)
36. Caldwell D. O., *Phys. Rev.*, **100**, 291 (1955)
37. Dalgarno, A., *Proc. Phys. Soc. (London), A*, **76**, 422 (1960)
38. Dalgarno, A., *Atomic and Molecular Processes*, 627 (Bates, D. R., Ed., Academic, New York, 1962)
39. Erskine, G. A., *Proc. Phys. Soc. (London), A* **67**, 640 (1954)
40. Fano, U., *Phys. Rev.*, **92**, 328 (1953)
41. Fano, U., *Phys. Rev.*, **95**, 1198 (1954)
42. Fano, U., *Phys. Rev.*, **102**, 385 (1956)
43. Fano, U., *Phys. Rev.*, **103**, 1202 (1956)
44. Fano, U., *Phys. Rev.*, **118**, 451 (1960)

45. Fermi, E., *Phys. Rev.*, **57,** 485 (1940); for a summary and later references see Uehling, E. A., *Ann. Rev. Nucl. Sci.*, **4,** 315 (1954)
46. Ferrell, R. A., *Phys. Rev.*, **107,** 450 (1957); Ferrell, R. A., and Quinn, J. J., *Phys. Rev.*, **108,** 570 (1957); Stern, E. A., and Ferrell, R. A., *Phys. Rev.*, **120,** 130 (1960)
47. Ferrell, R. A., *Phys. Rev.*, **111,** 1214 (1958)
48. Frank, A. L., Arakawa, E. T., and Birkhoff, R. D., *Phys. Rev.*, **126,** 1947 (1962)
49. Fröhlich, H., and Pelzer, H., *Proc. Phys. Soc.* (*London*), *A*, **68,** 525 (1955)
50. Galanin, M. D., *Opt. Spektroskopiya*, **4,** 758 (1958)
51. Ginzburg, V. L., and Frank, J. M., *Zh. Eksperim. Teor. Fiz.*, **16,** 15 (1946)
52. Gombás, P., *Encyclopedia of Physics*, **36/2,** 183 (Fluegge, S., Ed. Springer, Berlin, 1956)
53. Haeberli, W., Huber, P., and Baldinger, E., *Helv. Phys. Acta*, 26, 145 (1953)
54. Hahn, B., and Hughentobler, E., *Nuovo Cimento*, **17,** 983 (1960)
55. Halpern, O., and Hall, H., *Phys. Rev.*, **73,** 477 (1948)
56. Henneberg, W., *Z. Physik*, **86,** 592 (1933)
57. Hubbard, J., *Proc. Phys. Soc.* (*London*), *A*, **68,** 976 (1955)
58. Jensen, H., *Z. Physik*, **106,** 620 (1937)
59. Jesse, W. P., and Sadauskis, J., *Phys. Rev.*, **90,** 1120 (1953)
60. Jesse, W. P., and Sadauskis, J., *Phys. Rev.*, **107,** 766 (1957)
61. Jesse, W. P., *Phys. Rev.*, **109,** 2002 (1958)
62. Jesse, W. P., *Radiation Res.*, **13,** 1 (1960)
63. Jesse, W. P., and Platzman, R. L., *Nature*, **195,** 790 (1962); also Jesse, W. P., *J. Chem. Phys.*, **3,** 2774 (1963); Platzman, R. L., *J. Chem. Phys.*, **38,** 2775 (1963)
64. Kenney, V. P., *Phys. Rev.*, **119,** 432 (1960)
65. Koch, L., Messier, J., and Valin, J., *IRE Trans. Nucl. Sci.*, **NS8** (1), 43 (1961)
66. Kramers, H. A., *Physica*, **13,** 401 (1947)
67. Kronig, R., and Korringa, J., *Physica*, **10,** 406 (1943); **15,** 667 (1949)
68. Landau, L., *J. Phys.* (*USSR*), **8,** 201 (1944)
69. LaVilla, R., and Mendlowitz, H., *Phys. Rev. Letters*, **9,** 149 (1962)
70. Lewis, H. W., *Phys. Rev.*, **78,** 526 (1950)
71. Lewis, H. W., *Phys. Rev.*, **85,** 20 (1952)
72. Lindhard, J., and Scharff, M., *Kgl. Danske Videnskab. Selskab., Mat.-Fys. Medd.*, **27** (15) (1953)
73. Livingston, M. S., and Bethe, H. A., *Rev. Mod. Phys.*, **9,** 282–83 (1937)
74. McClure, G. W., *Phys. Rev.*, **90,** 796 (1953)
75. McKenzie, J. M., and Bromley, D. A., *Proc. Inst. Elec. Engrs.* (*London*), *B*, **106,** Suppl. 16, 731 (1959)
76. Martin, F. W., and Northcliffe, L. C., *Phys. Rev.*, **128,** 1166 (1962)
77. Marton, L., Leder, L. B., and Mendlowitz, H., *Advan. Electron. Electron Phys.*, **7,** 183 (1955)
78. Mather, R., and Segrè, E., *Phys. Rev.*, **84,** 191 (1951)
79. Mayer, J. W., *J. Appl. Phys.*, **30,** 1937 (1959)
80. Merzbacher, E., and Lewis, H. W., *Encyclopedia of Physics*, **34/2,** 166 (Fluegge, S., Ed., Springer, Berlin, 1958)
81. Messelt, S., *Nucl. Phys.*, **5,** 435 (1958)
82. Miller, W. F., *A Theoretical Study of Excitation and Ionization by Electrons in Helium and of the Mean Energy Per Ion Pair* (Doctoral thesis, Purdue Univ., Lafayette, Ind., 1956)
83. Molière, G., *Z. Naturforsch.*, **3a,** 78 (1948)
84. Murray, R. B., and Meyer, A., *IRE Trans. Nucl. Sci.*, **NS9** (3), 33 (1962)
85. *Penetration of Charged Particles in Matter, Natl. Acad. Sci.—Natl. Res. Council Publ. 752* (1960)
86. *Semiconductor Nuclear Particle Detectors*, especially pp. 91–98, 3–5, *Natl. Acad. Sci.—Natl. Res. Council Publ. 871* (1961)
87. *Penetration of Charged Particles in Matter, Natl. Acad. Sci.—Natl. Res. Council. Publ. 1133* (In preparation)
88. *Penetration of Charged Particles in Matter, Prelim. Rept. Natl. Acad. Sci.—Natl. Res. Council* (1962)
89. *Natl. Bur. Std.* (*U. S.*) *Handbook 79, Stopping Powers for Use with Cavity Chambers* (1961)
90. Neamtan, S. M., *Phys. Rev.*, **92,** 1362 (1953)
91. Northcliffe, L. C., *Ann. Rev. Nucl. Sci.*, **13,** 67 (1963)
92. Nozières, P., and Pines, D., *Phys. Rev.*, **109,** 741, 762, 1062 (1958)

93. Patrick, J. W., and Barkas, W. H., *Nuovo Cimento, Suppl.*, **23,** 1 (1962)
94. Perlman, H. S., *Proc. Phys. Soc. (London), A,* **76,** 433, 623 (1960)
95. Placzek, G., *Phys. Rev.*, **86,** 377 (1952), Secs. 3ff
96. Platzman, R. L., *Symp. Radiobiol., Oberlin Coll., 1950* (1952)
97. Platzman, R. L., *J. Phys. Radium,* **21,** 853 (1960)
98. Platzman, R. L., *J. Appl. Radiation Isotopes,* **10,** 116 (1961)
99. Platzman, R. L., *Radiation Res.*, **17,** 419 (1962)
100. Platzman, R. L. (Private communication)
101. Platzman, R. L., and Miller, W. F. (To be published)
102. Powell, C. J., *Proc. Phys. Soc. (London), A,* **76,** 593 (1960)
103. Ritchie, R. H., *Phys. Rev.*, **106,** 874 (1957)
104. Ritchie, R. H., and Eldridge, H. B., *Phys. Rev.*, **126,** 1935 (1962)
105. Rossi, B., *High Energy Particles,* 29 ff. (Prentice Hall, New York, 1952)
106. Rybakov, B. V., *Zh. Eksperim. Teor. Fiz.*, **28,** 651 (1955) [Transl., *Soviet Phys. JETP,* **1,** 435 (1955)]
107. Scott, W. T., *Rev. Mod. Phys.*, **35,** 231 (1963)
108. Seb, Do In, *Zh. Eksper. Teor. Fiz.*, **43,** 121 (1962) [Transl., *Soviet Phys. JETP,* **16,** 87 (1963)]
109. Shapiro, M. M., *Encyclopedia of Physics,* **45,/2,** 345 (Fluegge, S., Ed., Springer, Berlin, 1958)
110. Shockley, W., *Czech. J. Phys., B,* **11,** 81 (1961)
111. Silin, V. P., and Fetisov, E. P., *Phys. Rev. Letters,* **7,** 374 (1961)
112. Snyder, H. S., and Scott, W. T., *Phys. Rev.*, **76,** 220 (1949)
113. Spencer, L. V., and Fano, U., *Phys. Rev.*, **93,** 1172 (1954)
114. Spencer, L. V., *Phys. Rev.*, **98,** 1597 (1955)
115. Spencer, L. V., and Coyne, J., *Phys. Rev.*, **128,** 2230 (1962)
116. Steinmann, W., *Phys. Rev. Letters,* **5,** 470 (1960)
117. Stern, E. A., *Phys. Rev. Letters,* **8,** 7 (1962)
118. Sternheimer, R. M., *Phys. Rev.*, **88,** 851 (1952)
119. Sternheimer, R. M., *Phys. Rev.*, **89,** 1148 (1953); **91,** 256 (1953); **93,** 1434 (1954)
120. Sternheimer, R. M., *Phys. Rev.*, **93,** 351 (1954)
121. Sternheimer, R. M., *Phys. Rev.*, **103,** 511 (1956)
122. Sternheimer, R. M., *Phys. Rev.*, **115,** 137 (1959) [Errata **124,** 2051 (1961)]
123. Sternheimer, R. M., *Phys. Rev.*, **117,** 485 (1960)
124. Sternheimer, R. M., *Phys. Rev.*, **118,** 1045 (1960)
125. Stiller, B., *IV Intern. Kolloq. Korpuskularphot., München, 1963*
126. Symon, K. R., *Fluctuations in Energy Loss by High Energy Charged Particles in Passing Through Matter* (Doctoral thesis, Harvard Univ., Cambridge, Mass., 1948)
127. Tauc, J., *Phys. Chem. Solids,* **8,** 219 (1959)
128. Thompson, T. J., *Effect of Chemical Structure on Stopping Power for High-Energy Protons, Univ. Calif. Radiation Lab. Rept. No. 1910* (1952)
129. Tsytovich, V. N., *Dokl. Akad. Nauk SSSR,* **144,** 310 (1962) [Transl., *Soviet Phys. "Doklady,"* **7,** 411 (1962)]; *Zh. Eksperim. Teor. Fiz.*, **43,** 1782 (1962) [Transl., *Soviet Phys. JETP,* **16,** 1260 (1963)]
130. Uehling, E. A., *Ann. Rev. Nucl. Sci.*, **4,** 315 (1954)
131. Valentine, J. M., and Curran, S. C., *Rept. Progr. Phys.*, **21,** 1 (1958)
132. van Heerden, P. J., *The Crystal Counter* (North-Holland, Amsterdam, 1945)
133. Vavilov, P. V., *Zh. Eksperim. Teor. Fiz.*, **32,** 920 (1957) [Transl., *Soviet Phys. JETP,* **5,** 749 (1957)]
134. Walske, M. C., *Phys. Rev.*, **88,** 1283 (1952) and **101,** 940 (1956); also *The Stopping Power of K and L Shell Electrons* (Doctoral thesis, Cornell Univ., Ithaca, N. Y., 1951)
135. Walters, W. L., Costello, D. G., Skofronick, J. G., Palmer, D. W., Kane, W. E., and Herb, R. G., *Phys. Rev. Letters,* **7,** 284 (1961) and *Phys. Rev.*, **125,** 2012 (1962); Palmer, D. W., Skofronick, J. G., Costello, D. G., Morsell, A. L., Kane, W. E., and Herb, R. G., *Phys. Rev.*, **130,** 1153 (1963); see also theoretical discussion by Lewis, H. W., *Phys. Rev.*, **125,** 937 (1962)
136. Westermark, T., *Phys. Rev.*, **93,** 835 (1954)
137. Whaling, W., *Encyclopedia of Physics,* **34/2,** 193 (Fluegge, S., Ed., Springer, Berlin, 1958)
138. Whyte, G. N., *Radiation Res.*, **18** 265 (1963)

139. Yang, C. N., *Phys. Rev.*, **84**, 599 (1951)
140. Yuan, L. C., and Wu, C. S., Eds., *Methods Exptl. Phys.*, **5**, Pt. A (1955)
141. Zhdanov, G. B., Tretyakova, M. I., Tsytovich, V. N., and Shcherbakova, M. N., *Zh. Eksperim. Teor. Fiz.*, **43**, 342 (1962) [Transl., *Soviet Phys. JETP*, **16**, 245 (1963)]
142. Sechi-Zorn, B., and Zorn, G. T., *Bubble Density in a Hydrogen Bubble Chamber, Brookhaven Natl. Lab. Rept. 5866* (1962); *Nuovo Cimento, Suppl.* (In press)
143. Zrelov, V. P., and Stoletov, G. D., *Zh. Eksperim Teor. Fiz.*, **36**, 658 (1959) [Transl., *Soviet Phys. JETP*, **9**, 461 (1959)]
144. Williamson, C., and Boujot, J. P., *Tables of Range and Rate of Energy Loss of Charged Particles of Energy 0,5 to 150 MeV Rappt. CEA 2189* (Centre Études Nucl. Saclay, France, 1962)
145. Tenner, A. G., *Nucl. Instr. Methods*, **22**, 1 (1963)